

Origins of archaeal tetraether lipids in sediments: Insights from radiocarbon analysis

Sunita R. Shah^{a,*}, Gesine Mollenhauer^b, Naohiko Ohkouchi^c,
Timothy I. Eglinton^d, Ann Pearson^a

^a Department of Earth and Planetary Sciences, Harvard University, 20 Oxford Street, Cambridge, MA 02138, USA

^b Alfred Wegener Institute for Polar and Marine Research, D-27570 Bremerhaven, Germany

^c Institute for Research on Earth Evolution, Japan-Agency for Marine-Earth Science and Technology, Yokosuka 237-0061, Japan

^d Department of Marine Chemistry and Geochemistry, Woods Hole Oceanographic Institution, Woods Hole, MA 02543, USA

Received 30 January 2008; accepted in revised form 23 June 2008; available online 8 July 2008

Abstract

Understanding the supply and preservation of glycerol dibiphytanyl glycerol tetraethers (GDGTs) in marine sediments helps inform their use in paleoceanography. Compound-specific radiocarbon measurements of sedimentary alkenones from multiple environments have been used to gain insight into processes that affect U_{37}^K paleotemperature reconstructions. Similar analyses are warranted to investigate how analogous processes affecting GDGTs impact TEX_{86} paleotemperatures. Here we present radiocarbon measurements on individual GDGTs from Bermuda Rise and Santa Monica Basin sediments and discuss the results in the context of previous studies of co-depositional alkenones and foraminifera. The ^{14}C contents of GDGTs and planktonic foraminifera in Bermuda Rise are very similar, suggesting a local source; and TEX_{86} -derived temperatures agree more closely with foraminiferal temperatures than do U_{37}^K temperatures. In contrast, GDGTs in Santa Monica Basin are depleted in ^{14}C relative to both alkenones and foraminifera, and TEX_{86} temperatures agree poorly with known surface water values. We propose three possible factors that could explain these results: (i) GDGTs may be labile relative to alkenones during advective transport through oxic waters; (ii) archaeal production deep in the water column may contribute ^{14}C -depleted GDGTs to sediments; and (iii) some GDGTs also may derive from sedimentary archaeal communities. Each of these three processes is likely to occur with varying relative importance depending on geographic location. The latter two may help to explain why TEX_{86} temperature reconstructions from Santa Monica Basin do not appear to reflect actual sea surface temperatures. Terrigenous GDGTs are unlikely to be major contributors to Bermuda Rise or Santa Monica Basin sediments, based on values of the BIT index. The results also indicate that the crenarchaeol regioisomer is governed by processes different from other GDGTs. Individual measurements of the crenarchaeol regioisomer are significantly depleted in ^{14}C relative to co-occurring GDGTs, indicating an alternative origin for this compound that presently remains unknown. Re-examination of the contribution of crenarchaeol regioisomer to the TEX_{86} index shows that it is a significant influence on the sensitivity of temperature reconstructions.

© 2008 Elsevier Ltd. All rights reserved.

1. INTRODUCTION

Archaea are found ubiquitously in the water column (e.g., DeLong, 1992; Fuhrman et al., 1992; Karner et al.,

2001; Herndl et al., 2005) and in the sediments (e.g., Vetriani et al., 1998; Vetriani et al., 1999; Teske et al., 2002) of the modern ocean. The record of archaea through geologic time is preserved by their characteristic membrane lipids, which are abundant in marine sediments since the Cretaceous (Kuypers et al., 2002; Schouten et al., 2003a). A significant correlation has been observed between the composition of particular archaeal lipids in modern surface sediments, the

* Corresponding author. Fax: +1 617 496 4387.

E-mail address: shah@fas.harvard.edu (S.R. Shah).

glycerol dibiphytanyl glycerol tetraethers (GDGTs, molecular structures in Fig. 1) and overlying sea surface temperature. This correlation has inspired a paleotemperature proxy, the TEX₈₆ index (Schouten et al., 2002). The correlation between sedimentary GDGTs and sea surface temperatures suggests that GDGTs found in sediments originate predominantly from surface waters. Although marine archaea are found at all depths in the water column, primary export of GDGTs to the sediments is thought to occur by processes that dominantly exist in the upper water column (e.g., consumption by zooplankton and packaging into fecal pellets (Schouten et al., 2002; Wakeham et al., 2003; Wuchter et al., 2006)).

There is a need for greater understanding of the many potential sources and processes that ultimately could affect the preserved GDGT assemblages, and the long-chain alkenones produced by haptophyte algae (Marlowe et al., 1984) may be good models to help understand these processes. Alkenone abundances are the basis of the U₃₇^{K'} paleotemperature index (Brassell et al., 1986). They have been demonstrated to be more resistant to degradation than other lipid biomarker compounds (Grimalt et al., 2000, and references therein). GDGTs also are thought to be relatively resistant to degradation because of their ether linkages and isoprenoid alkyl groups (Fig. 1) (Sinninghe Damsté et al., 2002a; Schouten et al., 2004).

Compound-specific radiocarbon measurements have been made on co-depositional alkenones and planktonic foraminifera from the sediments of the Bermuda Rise (Ohkouchi et al., 2002); the Benguela Upwelling System off Namibia (Mollenhauer et al., 2003); the Chilean Margin, off the coast of northwest Africa, the South China Sea (Mollenhauer et al., 2005); and Santa Barbara and Santa Monica Basins (Mollenhauer and Eglinton, 2007). The ¹⁴C content of planktonic foraminifera reflects the ¹⁴C content of dissolved inorganic carbon (DIC) in surface seawater. Due to their large size and density, they are thought to settle directly to the seafloor and reflect the true depositional age of the sediment. Because haptophyte algae also incorporate DIC from surface seawater, alkenone and foraminiferal ¹⁴C contents would be identical if their export and burial processes were the same. However, alkenones generally are found to be depleted in ¹⁴C compared to planktonic foraminifera (Ohkouchi et al., 2002; Mollenhauer et al., 2003, 2005; Mollenhauer and Eglinton, 2007). This could result from various post-depositional processes such as bioturbation; the addition of pre-aged alkenones from an erosional source; or aging during resuspension, lateral transport and re-deposition from distant sediments. The largest ¹⁴C offsets between alkenones and planktonic foraminifera are found in the Bermuda Rise (Fig. 2, Ohkouchi et al., 2002), and the smallest offsets are from the South China Sea and off northwest Africa (Fig. 2,

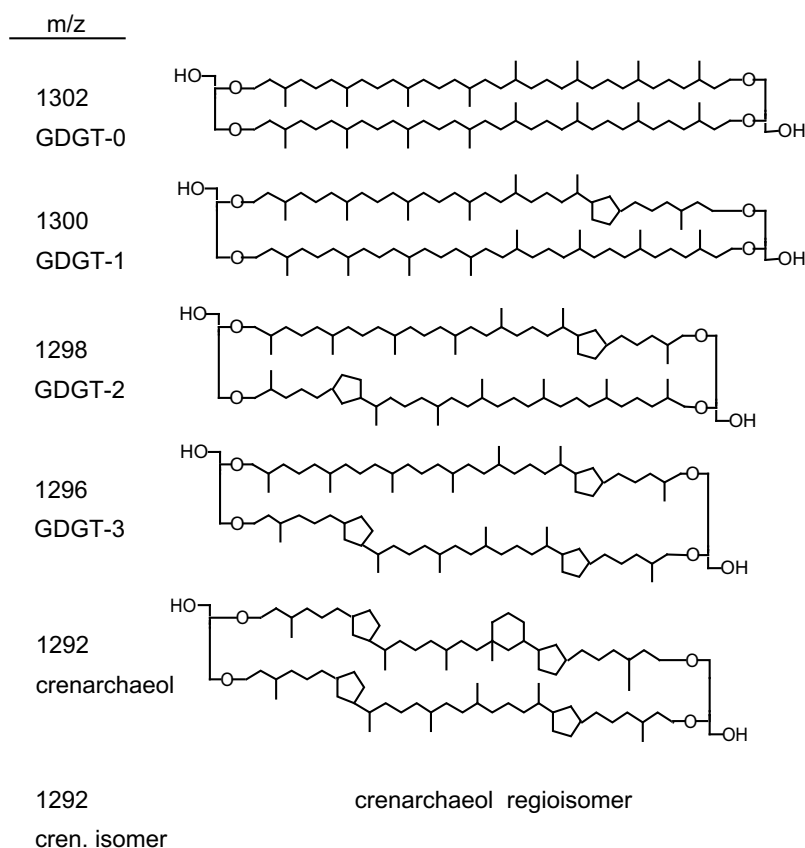


Fig. 1. Molecular masses, designations and molecular structures of five of the six most abundant GDGTs in Santa Monica Basin and Bermuda Rise sediments. The crenarchaeol regioisomer is a regioisomer of crenarchaeol (Sinninghe Damsté et al., 2002a,b).

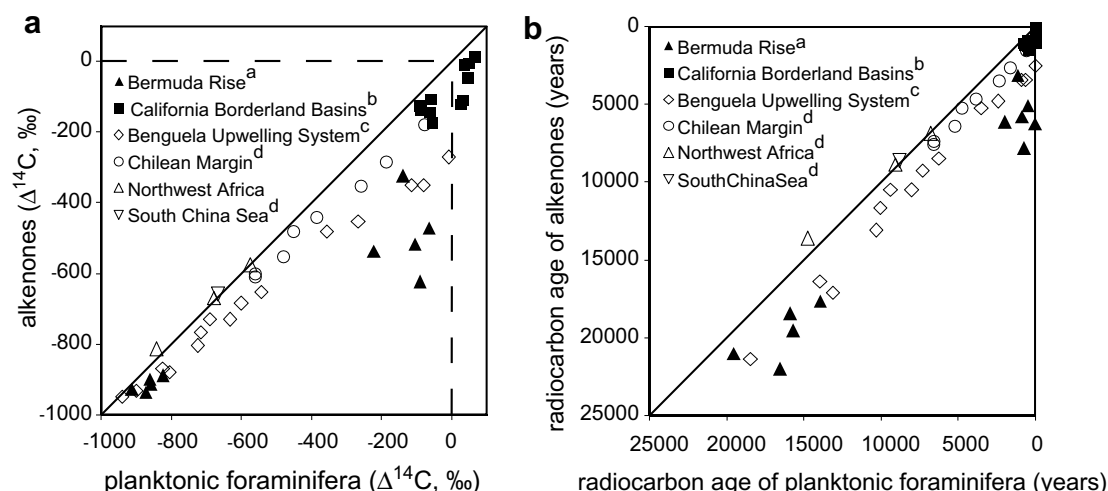


Fig. 2. Summary of published radiocarbon measurements of alkenones vs. planktonic foraminifera, expressed as (a) values of $\Delta^{14}\text{C}$ and (b) radiocarbon age. ^aData from Ohkouchi et al. (2002); $\Delta^{14}\text{C}$ values calculated from reported radiocarbon ages assuming all measurements made in 2000. ^bData from Mollenhauer and Eglinton (2007) with two additional values reported in this study; $\Delta^{14}\text{C}$ values calculated from reported fraction modern (f_{MC}); and corresponding planktonic foraminiferal radiocarbon measurements calculated from decay-corrected $\Delta^{14}\text{C}$ values reported in Pearson et al. (2000). ^cData from Mollenhauer et al. (2003); $\Delta^{14}\text{C}$ values calculated from reported percent modern (p_{MC}) values assuming all measurements made in 2001. ^dData from Mollenhauer et al. (2005); $\Delta^{14}\text{C}$ values calculated from reported f_{MC} values assuming all measurements made in 2003.

Mollenhauer et al., 2005). Multiple lines of evidence suggest that the primary control on the ^{14}C content of alkenones is the proportion of pre-aged alkenones delivered by lateral advective transport (Ohkouchi et al., 2002; Mollenhauer et al., 2003, 2005; Mollenhauer and Eglinton, 2007). The presumed source of this exogenous material is re-suspension from sediments originally deposited elsewhere. The recalcitrance of alkenone lipids, or potentially their intimate association either with coccolith biominerals or with the fine-grained clay mineral fraction of sediments, permits their survival over these distances. The relative proportion of the advected material from allochthonous sources is location-specific and determined by spatial variations in surface-water productivity, local bottom currents and sea-floor topography.

Like alkenones, archaeal GDGTs are large hydrophobic lipids and therefore also may associate with the fine-grained sediment fraction. Recently, radiocarbon measurements were reported for co-depositional alkenones, foraminifera, and in a subset of these samples, for the GDGT crenarchaeol (Fig. 2, Mollenhauer et al., 2007). Like alkenones, crenarchaeol appeared to show an age offset relative to planktonic foraminifera, offering preliminary evidence that crenarchaeol is indeed re-mobilized and advectively transported with bottom currents. However, the measurements also suggested that crenarchaeol may not be as resistant to degradation during transport in the nepheloid layer as alkenones, as crenarchaeol also appears to be less aged relative to alkenones with increasing transport time (Mollenhauer et al., 2007).

Determining the relative proportions of the various sources of GDGTs found in sediments is further complicated by the possibility that not all GDGTs are necessarily synthesized in the surface ocean. Archaea are abundant members of the total microbial community in the deep

water column (e.g., Karner et al., 2001; Herndl et al., 2005). Mesopelagic archaea, as well as populations living in the sediments, could contribute to the total pool of sedimentary GDGTs.

Here we report ^{14}C measurements for archaeal GDGTs obtained from the same Bermuda Rise and Santa Monica Basin samples for which alkenone and foraminiferal data are available (Pearson et al., 2000; Ohkouchi et al., 2002; Mollenhauer and Eglinton, 2007). These sites represent the locations having the largest (Bermuda Rise) and smallest (Santa Monica Basin, among sites with more than three alkenone measurements) ^{14}C offsets between corresponding planktonic foraminifera and alkenones (Fig. 2). The pattern of radiocarbon age offsets of GDGTs should indicate whether GDGTs are affected by re-suspension and advection processes over the same timescales as experienced by the alkenones found within identical sediments.

2. COMPARISON OF SETTINGS

Previous paleoceanographic studies have been conducted in both Bermuda Rise (e.g., Keigwin, 1996; Sachs and Lehman, 1999) and Santa Monica Basin sediments (Hagadorn et al., 1995; Christensen et al., 1996). Bermuda Rise is a North Atlantic sediment drift site where rapid accumulation results from advection and focusing of detrital material (Keigwin, 1996). Bermuda Rise sediments are oxic at the surface, and the rapid accumulation rate minimizes the effects of bioturbation and allows reconstruction of high-resolution paleoproxy records. However, a large fraction of the alkenones contributed to Bermuda Rise sediments by advection is thought to originate in the Canadian Margin off the coast of Nova Scotia (Ohkouchi et al., 2002). This advected detrital fraction contains alkenones having values of $U_{37}^{\text{K}'}$ reflecting formation in waters of colder sea

surface temperature (SST) and depleted ^{14}C contents (Ohkouchi et al., 2002); it also contains other lipid biomarkers (N. Ohkouchi, unpublished data).

Representing a very different setting, Santa Monica Basin (SMB) is part of the California Borderland Basin system. Its 905-m water column is suboxic below the sill depth of 740 m. High rates of organic matter preservation and laminated, anoxic sediments also allow paleoceanographic reconstructions with high temporal resolution (Hagadorn et al., 1995; Christensen et al., 1996). Very recently deposited material is preserved in the central SMB, as is evident from observations of bomb radiocarbon in planktonic foraminifera (Pearson et al., 2000; Mollenhauer and Eglinton, 2007) and alkenones (Mollenhauer and Eglinton, 2007). Bomb radiocarbon derived from nuclear bomb testing in the 1950s and 1960s is observed as a spike in the abundance of ^{14}C , and it therefore signals products derived from surface seawater over the last 50 years. It is found in the top 2.5 cm of sediment from the depositional center of Santa Monica Basin. However, like at Bermuda Rise, pre-aged organic material, including alkenones, also appears to be advectively delivered to the center of Santa Monica Basin (Mollenhauer and Eglinton, 2007). Here, the advected fraction of alkenones is thought to have been originally deposited on the adjacent California shelf (Mollenhauer and Eglinton, 2007).

3. EXPERIMENTAL

3.1. Sampling and lipid extraction

Archaeal GDGTs were isolated from archived lipid extracts obtained from cores previously processed for radiocarbon analysis of alkenones. Bermuda Rise samples are from cores BC9 (33°41.6'N, 57°36.7'W), GGC5 (33°41.5'N, 57°34.5'W) and GPC5 (33°41.2'N, 57°36.9'W) described in Ohkouchi et al. (2002). Total lipids were extracted, separated into acidic and neutral fractions and the neutral fraction was further separated into three polarity fractions (see Ohkouchi et al., 2005, for full method). For this study, the alcohol polarity fraction (eluted off SiO_2 column in chloroform (CH_2Cl_2)/methanol (MeOH) (95:5, v/v)) was further fractionated using Biotage Flash 12i pressurized chromatography (12 × 150 mm column, 32–63 μm particle size) into three sub-fractions eluting in hexane/ethyl acetate (EtOAc) (75:25, v/v), EtOAc, and MeOH (modified from fractions described in Pearson et al. (2001)). GDGTs were found in the fraction eluting in 100% EtOAc. Santa Monica Basin samples from 6–7 and 32–34 cm are from core SMB-900 (33°46.9'N, 118°49'W) previously described in Mollenhauer and Eglinton (2007). Total lipids were extracted and the alcohol/sterol fraction was obtained similarly to the process described for Bermuda Rise samples (Ohkouchi et al., 2005; Mollenhauer and Eglinton, 2007). The Santa Monica Basin samples from 1–2, 2–3 and 3–4 cm are from the Pulse-32 core (33°44.0'N, 118°50.0'W) previously described in Pearson et al. (2000, 2001). Total lipids were extracted and separated into polarity fractions using Biotage Flash pressurized chromatography by the process described above for Bermuda Rise samples.

3.2. GDGT isolation and purification

Individual GDGTs were isolated from polarity fractions using a two-step high-performance liquid chromatography (HPLC) method. Samples first are separated by normal-phase preparative HPLC (Smittenberg et al., 2002; Ingalls et al., 2006). Subsequently, each fraction is cleaned of co-eluting pigments by reverse-phase chromatography (Ingalls et al., 2006; Shah and Pearson, 2007). Compound identifications, peak elution times and relative abundances of GDGTs for each sample first were obtained by injecting 3–5% of the total sample and detecting the peaks by APCI-MS (Hopmans et al., 2000) monitoring m/z 1250–1350 for Santa Monica Basin samples and m/z 1000–1350 for Bermuda Rise samples. One Santa Monica Basin sample, from 6 to 7 cm sediment depth, was re-injected monitoring m/z 1000–1350. GDGTs then were isolated from the remainder of the sample by time-based fraction collection of between 6 and 9 individual HPLC injections. Before pooling, the contents of each time-based collection window were determined by flow injection analysis (FIA). The isolated GDGTs were pooled into four fractions: GDGT-0, GDGTs 1–3, crenarchaeol, and crenarchaeol regioisomer. GDGT numerical designations refer to the total number of cyclopentyl rings (Sinninghe Damsté et al., 2002b).

The normal-phase GDGT collections from all sediment depths and both locations were often colored green or brown, indicating co-elution of pigmented contaminants. GDGTs were purified of these contaminants by reverse-phase HPLC (Shah and Pearson, 2007) in one or two injections, depending on sample size. Purified GDGTs eluted over <2 min, and the contents of each collection were again verified by FIA. As each sample was processed with only one or two reverse-phase injections, each purified sample was collected in a maximum of 4 ml of running solvent. This has been shown to result in a minimal (0.03 $\mu\text{g}/\text{ml}$) process blank which is considerably less than the blank added by closed-tube combustion and other sample-preparation processes (Shah and Pearson, 2007). Aggregated fractions were colorless and dried to a white powder.

The expected carbon content of each sample was determined by comparing the FIA peak area to a correlation of the FIA peak area of previously processed samples and their carbon content as determined by quantification of CO_2 from combusted samples ($r^2 = 0.88$). The detection limit for GDGTs by this method is 0.3 μg of carbon (μgC). In most cases, samples estimated to have less than 25 μgC were combined with other GDGT fractions from the same sediment depth before combustion. For example, GDGT-0 (9 μgC), GDGT 1–3 (8 μgC), crenarchaeol (22 μgC) and crenarchaeol regioisomer (2 μgC) from 1 to 2 cm in Bermuda Rise were combined into a single ^{14}C measurement on 41 μgC .

Samples were transferred to quartz tubes, dried under ultra-pure N_2 , evacuated to 10^{-5} Torr, flame-sealed, and combusted according established methods. The resulting CO_2 was quantified and submitted to NOSAMS (<http://www.nosams.who.edu/>) for AMS measurement in 2006 and 2007.

3.3. AMS measurement and blank corrections

The size of samples submitted for radiocarbon measurement ranged from 6 to 219 μgC . All samples were processed using small-sample techniques (Pearson et al., 1998) as no sample had more than 300 μgC . The four samples isolated from 32 to 34 cm in Santa Monica Basin (GDGT-0, GDGTs 1–3, crenarchaeol, and crenarchaeol regioisomer) each had less than 25 μgC and were not combined before combustion. Because these samples would have had insufficient carbon for individual AMS measurement at NOSAMS, they were diluted with a known ratio of radiocarbon-dead CO_2 . Calculation of the corrected values of $\Delta^{14}\text{C}$ and the propagation of error associated with this dilution (Pearson et al., 1998) is described in Electronic Annex EA-1.

All samples were further corrected for sample processing blanks as described in Shah and Pearson (2007). This is particularly important for smaller samples as background carbon can contribute up to 2 μgC of the total sample. All radiocarbon values are reported here as values of $\Delta^{14}\text{C}$ (Stuiver and Polach, 1977). In most cases, these values have been corrected for fractionation effects using measured $\delta^{13}\text{C}$ values from the same sample. If $\delta^{13}\text{C}$ was not measured due to small sample size, $\delta^{13}\text{C}$ was assumed to be equal to an abundance-weighted average of other measurements from the same location and sediment depth. Values of $\Delta^{14}\text{C}$ were calculated from the NOSAMS-reported values of f_m following the conventions of Stuiver and Polach (1977):

$$\Delta^{14}\text{C} = (f_m * e^{\lambda * (1950 - y_m)} - 1) * 1000 \quad (1)$$

where $\lambda = 1/8267$ and y_m is the year measured.

Previously-measured values for alkenones and foraminifera from these cores were reported as conventional radiocarbon ages (Ohkouchi et al., 2002; Mollenhauer et al., 2003, 2005) or f_m values (Mollenhauer et al., 2003, 2005; Mollenhauer and Eglinton, 2007). To relate these reported values to the conventions used here, converted values of $\Delta^{14}\text{C}$ were calculated from f_m and/or from radiocarbon age (radiocarbon age = $-8033 * \ln(f_m)$, Stuiver and Polach, 1977). Alkenones and foraminifera from Bermuda Rise samples were assumed to have been measured in 2000. Adjusting these $\Delta^{14}\text{C}$ values for the additional decay that occurred between the year they were measured and the years our GDGTs were measured (2006–2007) would allow a more exact comparison of their radiocarbon contents. However, as this correction would have amounted to $\leq 1\text{‰}$, no correction was made. Foraminiferal $\Delta^{14}\text{C}$ values reported in Pearson et al. (2000) had been corrected for decay occurring since deposition to the sediment. This decay correction was removed for appropriate comparison with $\Delta^{14}\text{C}$ values in this study, which were not decay corrected.

3.4. Calculation of TEX_{86} and BIT index values

Values of the TEX_{86} index were calculated from relative abundances of GDGTs according to the equation defined in Schouten et al. (2002). Using our methods and HPLC instrument, the error associated with TEX_{86} values has previously been established at 0.01 TEX_{86} units. Branched and isoprenoid

tetraether (BIT) index values were also calculated according to Hopmans et al. (2004) for all sediment horizons of Bermuda Rise. It was only possible to measure the BIT index on one sediment horizon for Santa Monica Basin: 6–7 cm.

4. RESULTS

The lipid abundances of all samples had the characteristic marine archaeal GDGT profile: abundant GDGT-0 and crenarchaeol and smaller quantities of GDGT-1, GDGT-2, GDGT-3, and crenarchaeol regioisomer. Relative abundances are reported in Electronic Annex EA-2. TEX_{86} values were calculated based on these abundances (Schouten et al., 2002) and ranged from 0.54 to 0.72 in sediments from the Bermuda Rise (Table EA2-1). Using the most recent TEX_{86} calibration (Kim et al., 2008), these TEX_{86} values translate to temperatures between 20 and 30 $^\circ\text{C}$. TEX_{86} values calculated from Santa Monica Basin sediments were much more variable and ranged from 0.49 to 0.77 within just four centimeters of sediment depth. Despite their much more recent sediment ages (Fig. 3) (Mollenhauer and Eglinton, 2007), the temperatures reconstructed from these values were between 17 and 32 $^\circ\text{C}$ (Kim et al., 2008). BIT values for all sediment horizons from the Bermuda Rise were at or below 0.27 with an average value of 0.12. It was only possible to measure branched tetraether compounds on one sediment horizon from Santa Monica Basin: 6–7 cm. This BIT value was 0.16. These values fall within the range of open marine samples (Hopmans et al., 2004).

In sediments from the Bermuda Rise, archaeal GDGTs have values of $\Delta^{14}\text{C}$ that generally fall between the values for planktonic foraminifera and alkenones, although they are more similar to the foraminifera (Table 2 and Fig. 3a). The mass-weighted averages for total GDGTs are no more than 135‰ more ^{14}C -depleted than planktonic foraminifera, and sometimes are more ^{14}C -enriched (by up to 18‰). Below 6 cm sediment depth in particular, the offset between planktonic foraminiferal and average GDGT radiocarbon content is even smaller: the maximum ^{14}C -depletion for GDGTs relative to foraminifera is 28‰. In many horizons at these depths, the difference is less than the measurement uncertainty. When expressed in terms of radiocarbon years, the average age difference between GDGTs and foraminifera in the top 6 cm of the core is 950 ± 500 years. These horizons correspond to intervals with the greatest inferred input of advected material (N. Ohkouchi, unpublished data). Between 6 and 345 cm the offset is between 5 and 75 years, and below 350 cm it is between 440 and 2110 years.

The $\Delta^{14}\text{C}$ values of co-depositional planktonic foraminifera and alkenones also differ. However, in contrast to the GDGTs, when these alkenone-foraminiferal differences are expressed as radiocarbon ages, the offset does not change appreciably or systematically with depth (4000 ± 2000 years) and is larger than the difference between foraminifera and GDGTs (Ohkouchi et al., 2002). These results show that there must be different mechanisms

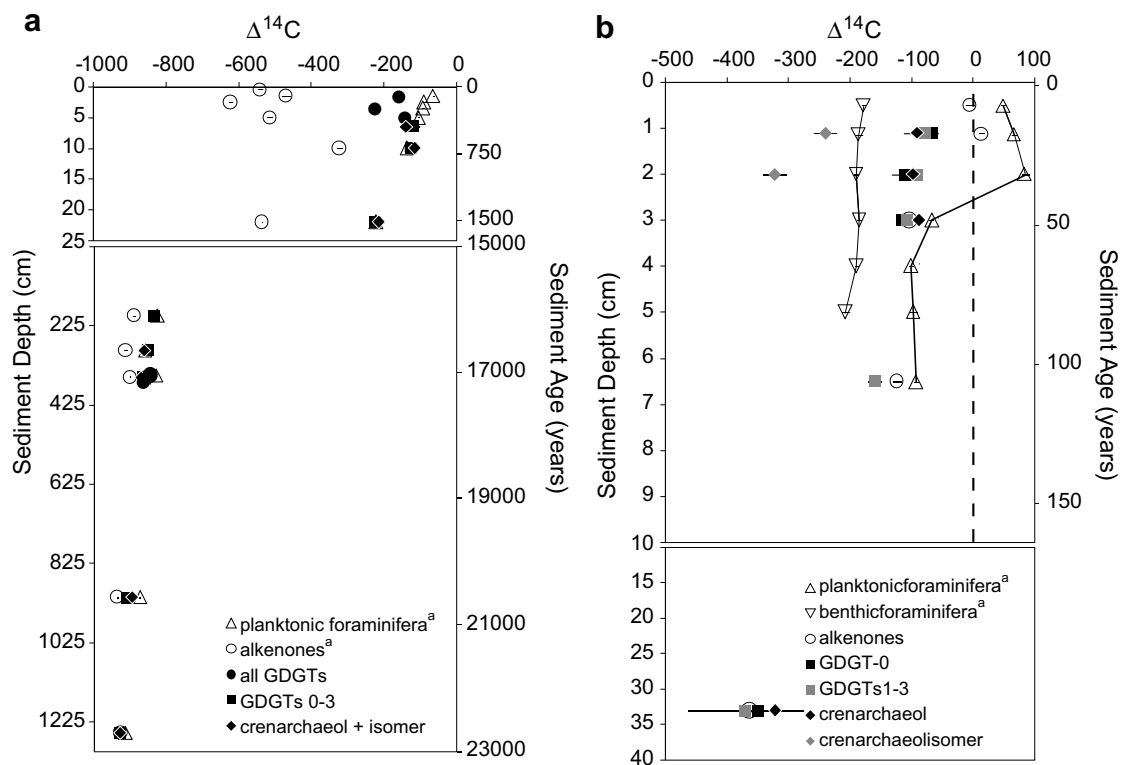


Fig. 3. (a) $\Delta^{14}\text{C}$ values from Bermuda Rise. Filled circles represent measurements made on all six GDGTs combined. Measurements made on combined GDGT-0, GDGT-1, GDGT-2 and GDGT-3 are represented by filled squares. Combined measurements of crenarchaeol plus crenarchaeol regioisomer are represented by filled diamonds. ^aValues of $\Delta^{14}\text{C}$ for alkenones and foraminifera (*G. ruber*) from Ohkouchi et al. (2002). (b) $\Delta^{14}\text{C}$ values from Santa Monica Basin. Measurements made on combined GDGT-1, GDGT-2 and GDGT-3 are represented by gray squares. Measurements of GDGT-0 (black squares), crenarchaeol (black diamonds), and crenarchaeol regioisomer (gray diamonds) were made on individual lipids. ^aValues of $\Delta^{14}\text{C}$ for alkenones and mixed planktonic foraminifera for sediment depths 0–1, 6–7 and 32–34 cm from Mollenhauer et al. (2007, core SMB-900). The $\Delta^{14}\text{C}$ values for GDGTs from depths 0–1, 6–7 and 32–34 cm also are from core SMB-900. The $\Delta^{14}\text{C}$ values for 0.75–1.5, 1.5–2.5, 2.5–3.5, 3.5–4.5, and 4.5–5.5 cm are from Pulse-32 core, originally described in Pearson et al. (2000). $\Delta^{14}\text{C}$ values for planktonic (*Neogloboquadrina* spp.) and benthic (*Bolivina* spp.) foraminifera calculated from decay-corrected values reported in Pearson et al. (2000). Alkenone values for core Pulse-32 are from this study. Horizontal error bars are total ^{14}C measurement errors (1σ) and in most cases are smaller than the size of the symbols.

controlling the ^{14}C contents of sedimentary GDGTs and alkenones in Bermuda Rise sediments.

In contrast to the patterns seen in Bermuda Rise, archaeal GDGTs from Santa Monica Basin generally are more depleted in ^{14}C compared to both foraminifera and alkenones (Table 2 and Fig. 3b), agreeing with data previously published for this location (Pearson et al., 2001). At each depth, the $\Delta^{14}\text{C}$ values of archaeal GDGTs fall between the $\Delta^{14}\text{C}$ values of the planktonic and benthic foraminifera. The notable exception is crenarchaeol regioisomer, which is significantly more depleted than any compound (Fig. 3b) other than petroleum-derived *n*-alkanes measured within these horizons (Pearson et al., 2000, 2001).

The abundance-weighted average of the other GDGTs (calculated without contribution from the anomalous crenarchaeol regioisomer) is more ^{14}C -depleted than planktonic foraminifera by between 30‰ and 160‰, with all of the individual differences being significant. The higher $\Delta^{14}\text{C}$ values in the planktonic foraminifera are greatly influenced by the bomb radiocarbon evident in the $\Delta^{14}\text{C}$ values from 0–0.75, 0.75–1.5 and 1.5–2.5 cm, and it would be inaccurate

to express the corresponding GDGT-foraminiferal differences in terms of radiocarbon years. But importantly, archaeal GDGTs do not show a detectable influence from bomb radiocarbon at any depth, with the possible exception of GDGT-0 from 0.75 to 1.5 cm depth (-67‰ , which is 15‰ higher than pre-bomb surface waters in this region). GDGTs also are more ^{14}C -depleted than co-depositional alkenones by up to 110‰, with some of the individual differences being significant and others within measurement errors. As with the GDGTs and planktonic foraminifera, this average difference is largest in the 0.75–1.5 cm horizon because of the bomb radiocarbon evident in the alkenones. In the pre-bomb sediment horizons, $\Delta^{14}\text{C}$ values of alkenones and GDGTs are within measurement error of each other, but in post-bomb horizons, GDGTs are significantly ^{14}C -depleted relative to alkenones. These patterns again show that the mechanisms that control the ^{14}C contents of alkenones and GDGTs must be different.

To decouple post-depositional processes from the effects of surface ocean conditions (e.g., surface ocean reservoir age and time-varying ^{14}C content), comparisons can be

made between the ^{14}C contents of foraminifera, alkenones and GDGTs within each sediment horizon. Plotting the $\Delta^{14}\text{C}$ values of alkenones and GDGTs relative to their co-occurring planktonic foraminifera shows characteristic relationships for Bermuda Rise (Fig. 4a) and Santa Monica Basin (Fig. 4b). The similarity between the $\Delta^{14}\text{C}$ values of GDGTs and planktonic foraminifera in Bermuda Rise is evident by the proximity of these samples to the 1:1 line (Fig. 4a). This contrasts with the relationship in Santa Monica Basin, where GDGTs plot significantly offset from the 1:1 line (Fig. 4b). The question then becomes whether such patterns are best explained by different sources or by post-depositional processes that affect the GDGTs and alkenones.

5. DISCUSSION

5.1. Processes with potential to cause a ^{14}C offset

Multiple mechanisms could be invoked to explain why the pre-aged component of sedimentary alkenones is not the same as the pre-aged component of sedimentary GDGTs. The production and export of alkenones is greater over the Nova Scotian Margin (the source of advectively delivered material to the Bermuda Rise) compared to the Sargasso Sea. This difference enhances the importance of advectively delivered alkenones relative to the supply of locally sourced alkenones at Bermuda Rise (Ohkouchi et al., 2002). Although analogous differences in GDGT production have not been quantified, Crenarchaeota are found throughout the oceans, and the distant advective source may not dominate GDGT sources in the same way.

GDGTs also may be more labile than alkenones. Alkenones are offset from planktonic foraminifera by up to 7100 years at Bermuda Rise (Ohkouchi et al., 2002); GDGTs may degrade during transport over such long temporal histories, effectively increasing the importance of local sources. In contrast, GDGTs may survive the shorter timescale of

transport processes in Santa Monica Basin (alkenone-foraminifera offset up to 430 years; Mollenhauer and Eglinton, 2007). Although degradation could help to explain the general absence of ^{14}C -depleted GDGTs at Bermuda Rise, this mechanism predicts that GDGTs would have ^{14}C contents similar to alkenones at Santa Monica Basin. Because they do not, anomalously aged source(s) of GDGTs are also required to explain the depletion in ^{14}C . Lability effects alone cannot cause GDGTs to be more ^{14}C -depleted than alkenones. GDGTs could be contributed to Santa Monica Basin by archaea that incorporate ^{14}C -depleted DIC from the deep, suboxic water column. Alternatively, archaeal communities living within anoxic, organic-rich Santa Monica Basin sediments could be synthesizing GDGTs from old sedimentary carbon substrates. Finally, it is possible that there could be contributions of pre-aged GDGTs from terrestrial sources, because of the greater proximity to continental runoff than at Bermuda Rise. Each of these options is discussed below.

5.1.1. Preferential degradation of GDGTs during lateral advection

Detrital material contributed to Bermuda Rise sediments is thought to originate from the Canadian Margin, off the coast of Nova Scotia (Keigwin, 1996; Ohkouchi et al., 2002). This region experiences abundant production of haptophyte algae; and as indicated by the radiocarbon age of alkenones delivered to Bermuda Rise, ~ 7000 years pass between production and final deposition (Fig. 2; Ohkouchi et al., 2002). In contrast, in the depositional centers of the California Borderland Basins, the age offset between planktonic foraminifera and alkenones is only 340 ± 60 years (calculated from pre-bomb sediment horizons only, Mollenhauer and Eglinton, 2007). This smaller age offset reflects a much more proximal and rapid source for delivery of alkenones: local transport from the adjacent California shelf (Mollenhauer and Eglinton, 2007).

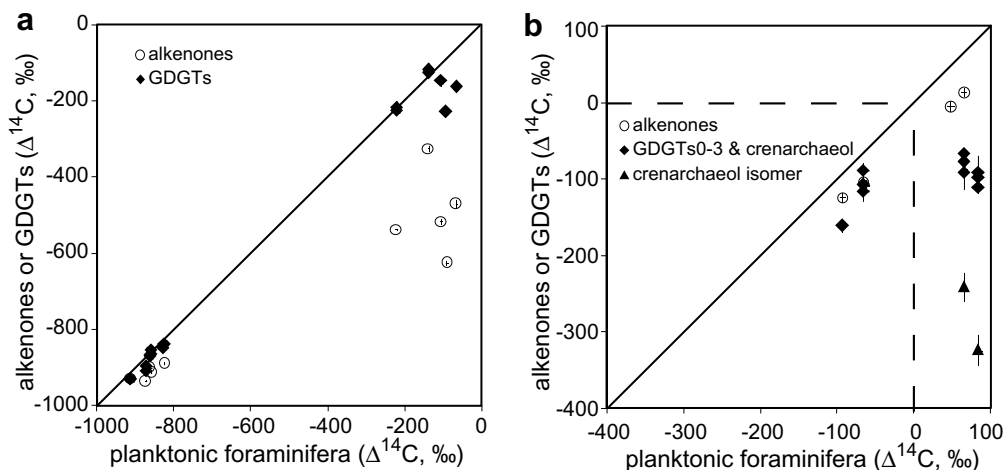


Fig. 4. $\Delta^{14}\text{C}$ values of alkenones and GDGTs vs. planktonic foraminifera for Bermuda Rise (a) and Santa Monica Basin (b). Individual GDGTs measurements from the same sediment depth are plotted separately; however replicate alkenone measurements (Mollenhauer and Eglinton, 2007) are averaged. Samples having values of $\Delta^{14}\text{C}$ greater than -84‰ contain bomb radiocarbon. Error bars represent 1σ measurement uncertainties in $\Delta^{14}\text{C}$ values.

Patterns of GDGT ages do not conform to the above patterns observed for alkenones. These differences could be partially caused by unequal lability. Alkenones are more resistant to degradation than many other lipids (Grimalt et al., 2000, and references therein). Limited information exists about the recalcitrance of GDGTs relative to each other, to alkenones, or to other lipid biomarkers (Sinninghe Damsté et al., 2002a; Schouten et al., 2004; Huguet, 2007). If GDGTs are preferentially degraded during advection through an oxic nepheloid layer, the contribution of exogenous GDGTs would be reduced as a function of transport time and distance. Large radiocarbon offsets between alkenones and foraminifera would indicate a long time spent in re-suspension. This would in turn correspond to smaller radiocarbon offsets between GDGTs and foraminifera, because the contribution from advected GDGTs would be minimal and most GDGTs would be local. Indeed, at Bermuda Rise, the average difference between the radiocarbon ages of GDGTs and foraminifera (820 ± 800 years) is much smaller than the difference between alkenones and foraminifera (4000 ± 2000 years).

In Santa Monica Basin where the delay between surface export and burial is short, and alkenone sources are primarily local, the radiocarbon ages of GDGTs and alkenones would be expected to be within measurement errors, and both would be <400 years different from foraminifera. It is therefore surprising that the GDGT-foraminifera offset generally is larger and much more variable (275–630 years for pre-bomb depths, or 1280–1600 years for post-bomb depths; Fig. 4). These older ages indicate that additional influences on the sedimentary GDGT pool are also required in Santa Monica Basin.

Observations from the Benguela Upwelling System are consistent with the hypothesized lability of GDGTs (Mollenhauer et al., 2007). Radiocarbon contents of crenarchaeol, alkenones, and planktonic foraminifera from two transects across the continental shelf indicated that crenarchaeol is more rapidly degraded than alkenones. Like our results for Bermuda Rise, a smaller fraction of pre-aged crenarchaeol contributed to the sediments farther downslope on the continental margin, which in this case is also increased transport distance. In the Benguela Upwelling System, alkenones often have the largest radiocarbon age offset of all measured components relative to foraminifera (Mollenhauer et al., 2003, 2007). The more labile short-chain fatty acids are very slightly different from planktonic foraminiferal ages (Mollenhauer et al., 2003). Although a direct comparison between fatty acids, alkenones, and crenarchaeol cannot be made within any single sediment horizon from these data, it appears that crenarchaeol has an intermediate age that falls between the (old) alkenones and the (young) fatty acids (Mollenhauer et al., 2003, 2007). This implies that GDGTs in the Benguela Upwelling System have an intermediate degree of lability.

However, direct evidence about the degradation potential of GDGTs is limited, and previous assessments of the relative lability of GDGTs have yielded contradictory results. Sinninghe Damsté et al. (2002a,b) compared abundances of alkenones, GDGTs, and other lipid biomarkers in sediment cores from three locations in the Arabian

Sea. These cores were geographically proximal, but from different water column depths (920, 1470 and 3001 m). Presumably, all three cores experienced similar overlying surface water conditions and export production, but had varying bottom water oxygen concentrations. A comparison of alkenones and GDGTs in both anoxic and oxic samples showed greater preservation of alkenones in some cores and greater preservation of GDGTs in others (Sinninghe Damsté et al., 2002a). These data suggested that both compound classes have similar resistance to degradation, although it also is possible that downslope sediment transport could have affected the results. Alkenone and GDGT preservation efficiencies >100% indicate material was added to the 1470 and 3001 m sites by advection of sediments (Sinninghe Damsté et al., 2002a). A similar result was reported in a study of organic-rich turbidite sediments from the Madeira Abyssal Plain (Huguet, 2007). In most instances, the C₃₇ alkenone preservation efficiency was slightly higher than the preservation efficiencies of individual archaeal GDGTs. However, there were exceptions where the alkenone preservation efficiency was slightly lower than GDGT preservation efficiency and one instance where it was much higher. These results may again suggest comparable lability between alkenones and GDGTs, although both cases are affected by an undetermined amount of exposure to oxygen while on the continental shelf. These results are not compatible with radiocarbon data discussed above and are not easily explained.

Mollenhauer et al. (2007) have shown that alkenones and GDGTs are re-suspended from sediments and transported across the Namibian continental shelf. During this process, GDGTs are degraded more quickly than alkenones and GDGTs increasingly reflect a local surface export source while alkenones are a combination of local and laterally advected material. These results are more compatible with our radiocarbon data, although may be inconsistent with the results based on concentration data alone (Sinninghe Damsté et al., 2002a; Huguet, 2007).

Assessing the degradation of alkenones and GDGTs in sinking particulate organic matter (POM) within the water column is complicated by the fact that GDGT production is not limited to surface waters. However, mesopelagic archaea generally are thought to be free-living (DeLong et al., 1993; Woebken et al., 2007), and most evidence suggests that sediment traps selectively accumulate archaeal biomass associated with POM sinking from the surface (Wuchter et al., 2006; Huguet et al., 2007). The accumulation rate of alkenones and GDGTs has been measured in sediment traps at 1500 and 3000 m in the Arabian Sea. An average of 25% of the GDGT flux survives transport from 1500 to 3000 m (Wuchter et al., 2006) compared to 55–65% preservation of alkenone flux between approximately the same depths (Wakeham et al., 2002). These data also suggest that GDGTs are preferentially degraded relative to alkenones when degradation specifically is occurring in an oxic water column.

Our TEX₈₆ sea surface temperature reconstructions from Bermuda Rise also support this interpretation.

TEX₈₆-calculated temperatures (Fig. 5) have a similar general pattern as the SSTs derived from foraminiferal $\delta^{18}\text{O}$ values (Keigwin, 1996). Although our values are offset with a bias towards warmer SSTs (by approximately 2 °C), they mirror the foraminiferal temperatures much more accurately than do the alkenone temperatures from these horizons. The U_{37}^K temperatures support the interpretation of a fractional contribution of alkenones from colder waters (Ohkouchi et al., 2002), while our results suggest that both GDGTs and planktonic foraminifera have primarily local sources. This is consistent with a contribution of alkenones but not of GDGTs within the fine-grained fraction that arrives from the Canadian Margin. Such a hypothesis also would predict that the largest differences between the $\Delta^{14}\text{C}$ values of alkenones and GDGTs should correspond with the largest differences between the U_{37}^K and TEX₈₆ temperature reconstructions. Our data agree, showing a weak relationship within a wide degree of scatter that suggests this is not the only factor affecting the accumulation of GDGTs.

In summary, three lines of evidence—radiocarbon values, sediment trap studies, and temperature reconstructions—support preferential degradation of GDGTs compared to alkenones under oxic conditions. However, results from sediment cores (Sinninghe Damsté et al., 2002a; Huguet, 2007) in some cases may be contradictory. Regardless, the apparent differential lability cannot explain how GDGTs can become more ^{14}C -depleted than associated alkenones.

5.1.2. Contribution of GDGTs exported from deep in the water column

5.1.2. Contribution of GDGTs exported from deep in the water column

Crenarchaeota are found at all depths in the marine water column (e.g., Karner et al., 2001; Herndl et al., 2005). They primarily are believed to be autotrophs (Wuchter et al., 2003; Herndl et al., 2005; Könneke et al., 2005), and $\Delta^{14}\text{C}$ values of their GDGTs closely parallel the ^{14}C content of DIC (Pearson et al., 2001; Ingalls et al., 2006). Because the ^{14}C content of DIC decreases with depth, GDGTs produced by archaea in the deep water column are more ^{14}C -depleted relative to GDGTs produced in surface waters (Ingalls et al., 2006). This process could deliver anomalously old GDGTs to sediments and potentially could explain how $\Delta^{14}\text{C}$ values of GDGTs in some cases are more negative than values from corresponding alkenones.

Mechanistically, however, this is a difficult hypothesis to reconcile. Export from the sea surface, where grazing incorporates lipids into sinking POC, is supported by particulate flux studies and by TEX₈₆ temperature reconstructions (e.g., Schouten et al., 2002; Wuchter et al., 2006). A similarly efficient packaging and transport mechanism for export of GDGTs from the deeper water column has not been identified, and sub-surface export of GDGTs is not expected to contribute significantly to the sedimentary GDGT pool in most locations.

However, recent evidence suggests that such an unidentified mechanism could exist. In a study of GDGT fluxes in Santa Barbara Basin, Huguet et al. (2007) concluded that the TEX₈₆ temperature recorded in a deep-water sediment trap (TEX₈₆ temperatures 8–12 °C) reflected a GDGT lipid flux from variable depths below 75 m rather than from the surface (12–21 °C). This was interpreted in terms of a single depth of export production that intermittently shoaled and deepened (Huguet et al., 2007). These results could equally be interpreted, however, as reflecting an integrated signal exported from a large but variable fraction of the entire water column.

To explore the potential magnitude of sub-surface export, we used a two end-member model. It treats sedimentary GDGTs as a mixture of material derived from two sources: the water column and a pre-aged source. The latter could be interpreted as lateral advection of sedimentary GDGTs, local benthic production, or a combination of these sources. The $\Delta^{14}\text{C}$ value of the water column fraction reflects DIC at the modeled depth(s) of export, and the $\Delta^{14}\text{C}$ value and fractional contribution of the pre-aged source is assumed to be constant with time. Total sedimentary GDGTs therefore would be represented by:

$$\Delta_{\text{GDGT}} = f * \Delta_{\text{water column}} + (1 - f) * \Delta_{\text{pre-aged}} \quad (2)$$

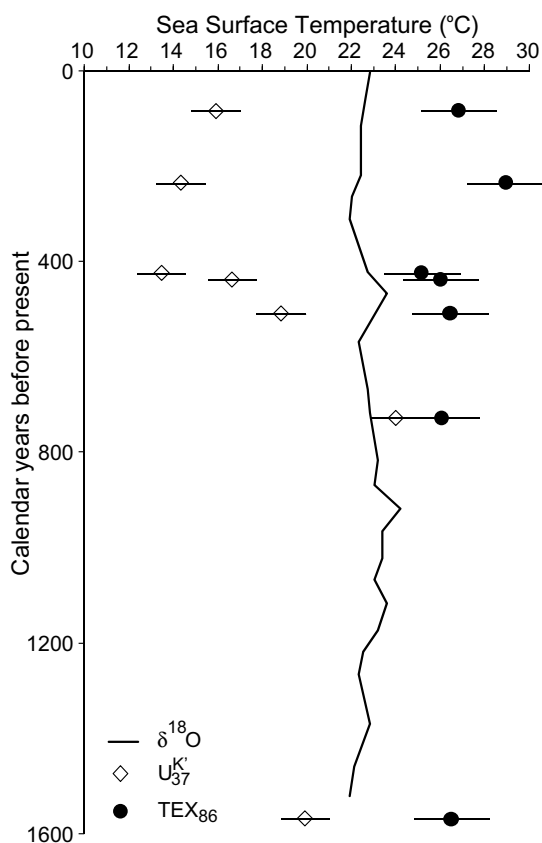


Fig. 5. Paleotemperature proxy reconstructions for Bermuda Rise plotted against sediment age. Sea surface temperatures calculated from $\delta^{18}\text{O}$ reported in Keigwin (1996), U_{37}^K values from Ohkouchi et al. (2002) converted to sea surface temperature using the most recent calibration of Conte et al. (2006) with an error of 1.2 °C. TEX₈₆-temperature reconstructions calculated using calibration of Kim et al. (2008) with an error of 1.7 °C.

Table 1
 $\delta^{13}\text{C}$ and $\Delta^{14}\text{C}$ values of GDGTs from Bermuda Rise and Santa Monica Basin

| Location | Core | Sediment depth (cm) | GDGTs in sample | Sample size (μgC) | $\delta^{13}\text{C}$ (‰) | $\Delta^{14}\text{C}$ (‰) | $\Delta^{14}\text{C}$ (\pm) |
|--------------------|-----------|-------------------------|-------------------------|--------------------------------|---------------------------|---------------------------|---------------------------------|
| Bermuda Rise | BC9C | 0–1 | All | 3 | Insufficient carbon | | |
| | BC9C | 1–2 | All | 41 | –19.4 | –163 | 16 |
| | BC9C | 3–4 | All | 76 | –18.5 | –228 | 12 |
| | BC9C | 4–6 | All | 51 | –18.5 | –146 | 15 |
| | BC9 | 6–7 | GDGTs 0–3 | 31 | | –121 | 18 |
| | BC9 | 6–7 | Crenarchaeol and isomer | 50 | –18.1 | –140 | 20 |
| | BC9 | 9–11 | GDGTs 0–3 | 46 | –18.2 | –125 | 11 |
| | BC9 | 9–11 | Crenarchaeol and isomer | 33 | | –117 | 17 |
| | BC9 | 21–23 | GDGTs 0–3 | 61 | –18.3 | –223 | 11 |
| | BC9 | 21–23 | Crenarchaeol and isomer | 41 | –18.5 | –215 | 15 |
| | GGC5 | 192–206 | GDGTs 0–3 | 84 | –18.2 | –837 | 6 |
| | GGC5 | 282–292 | GDGTs 0–3 | 40 | | –852 | 11 |
| | GGC5 | 282–292 | Crenarchaeol and isomer | 85 | –17.9 | –863 | 5 |
| | GGC5 | 350–360 | GDGTs 0–3 | 30 | | –866 | 14 |
| | GGC5 | 350–360 | Crenarchaeol and isomer | 68 | –18.5 | –870 | 6 |
| | GGC5 | 360–372 | All | 55 | –19.7 | –866 | 8 |
| | GPC5 | 345–355 | All | 33 | –18.8 | –848 | 11 |
| | GPC5 | 907–912 | GDGTs 0–3 | 33 | | –909 | 11 |
| | GPC5 | 907–912 | Crenarchaeol and isomer | 49 | –19.0 | –894 | 8 |
| | GPC5 | 1244–1260 | GDGTs 0–3 | 102 | –19.6 | –928 | 6 |
| GPC5 | 1244–1260 | Crenarchaeol and isomer | 87 | –18.5 | –929 | 6 | |
| Santa Monica Basin | Pulse-32 | 0–0.75 | All | | Insufficient carbon | | |
| | Pulse-32 | 0.75–1.5 | GDGT-0 | 134 | –18.4 | –67 | 7 |
| | Pulse-32 | 0.75–1.5 | GDGTs 1–3 | 69 | –19.1 | –77 | 10 |
| | Pulse-32 | 0.75–1.5 | Crenarchaeol | 219 | | –91 | 22 |
| | Pulse-32 | 0.75–1.5 | Crenarchaeol isomer | 20 | –20.6 | –241 | 19 |
| | Pulse-32 | 1.5–2.5 | GDGT-0 | 173 | –19.2 | –111 | 9 |
| | Pulse-32 | 1.5–2.5 | GDGTs 1–3 | 73 | –18.9 | –106 | 10 |
| | Pulse-32 | 1.5–2.5 | Crenarchaeol | 131 | –19.0 | –98 | 9 |
| | Pulse-32 | 1.5–2.5 | Crenarchaeol isomer | 25 | | –323 | 20 |
| | Pulse-32 | 2.5–3.5 | GDGT-0 | 27 | –19.8 | –116 | 13 |
| | Pulse-32 | 2.5–3.5 | GDGTs 1–3 | 70 | –18.8 | –108 | 7 |
| | Pulse-32 | 2.5–3.5 | Crenarchaeol | 86 | | –88 | 9 |
| | SMB-900 | 6–7 | GDGTs 1–3 | 69 | –19.0 | –161 | 9 |
| | SMB-900 | 32–34 | GDGT-0 | 6 | –21.4 | –350 | 75 |
| | SMB-900 | 32–34 | GDGTs 1–3 | 9 | | –370 | 93 |
| | SMB-900 | 32–34 | Crenarchaeol | 15 | | –321 | 31 |

where f is the fraction of the sedimentary GDGT pool derived from the water column. Both f and $\Delta_{\text{pre-aged}}$ are unknown, but this equation can be solved for pre-bomb and post-bomb conditions. This allows determination of both unknowns.

Two cases were examined: (i) export of GDGTs from the surface ocean (0–75 m) and (ii) export of GDGTs from below 75 m in the water column. Input parameters are summarized in Table 3. Decay-corrected values of $\Delta^{14}\text{C}$ from planktonic foraminifera define the local ^{14}C content of surface water DIC in both post-bomb and pre-bomb conditions ($\Delta_{\text{water-column}}$, case (i), Table 3; Pearson et al., 2000). The post-bomb and pre-bomb $\Delta^{14}\text{C}$ profiles of DIC below 75 m in the water column were estimated from the WOCE profile for station 10 of line P17C (Tsuchiya, 2000; Table 3). For case (ii), an equal abundance of GDGTs was assumed to be exported from all depths >75 m, and a depth-integrated average $\Delta^{14}\text{C}$ value was calculated from the DIC profile ($\Delta_{\text{water-column}}$, case (ii), Table 3). For both cases (i) and (ii), the mass-weighted average of decay-corrected $\Delta^{14}\text{C}$ measurements was used for Δ_{GDGT} .

Solving the mass balance for case (i) allows between 0% and 26% of GDGTs to derive from surface waters (0–75 m). The remainder would derive from the pre-aged (advective or benthic) source, which would have an average $\Delta^{14}\text{C}$ value of -122‰ . In the case of uniform export from below 75 m depth (case (ii)), the values of $\Delta^{14}\text{C}$ for the deep water column and for the measured sedimentary GDGTs are so similar that up to 100% of the GDGTs in the sediment could come from 75 to 900 m in the water column ($f = 0.51 \pm 0.5$). The separate pre-aged source, if there is one, would have an average $\Delta^{14}\text{C}$ value of -107‰ . It is not possible to distinguish which is the correct option in case (ii), but it is evident that if GDGT export flux derives entirely from the surface (case (i)), then nearly all of the GDGTs in SMB sediments are either detrital or from production in the sediments. This is supported by the absence of an observable bomb-radiocarbon signal in GDGTs from 0 to 2.5 cm in Santa Monica Basin sediment, in agreement with previous results (Pearson et al., 2001). And in both cases, the

Table 2
Summary of $\Delta^{14}\text{C}$ values calculated from previous results and measured in this study

| Core | Sediment depth (cm) | $\Delta^{14}\text{C}$ (‰) | | | | | | | |
|--------------------|---------------------|---------------------------|----------------------|-----------------|------------------------------------|---------------|---------------|---------------------------------|---------------------------------|
| | | Planktonic foraminifera | Benthic foraminifera | Alkenone | GDGT-0 | GDGTs 1–3 | Crenarchaeol | Crenarchaeol isomer | Abundance-weighted GDGT average |
| Santa Monica Basin | | | | | | | | | |
| Pulse-32 | 0.75–1.5 | 64 ± 4^a | -188 ± 6^a | 12 ± 5 | -67 ± 7 | -77 ± 10 | -91 ± 22 | -241 ± 19 | -93 |
| Pulse-32 | 1.5–2.5 | 81 ± 6^a | -194 ± 3^a | | -111 ± 9 | -106 ± 10 | -98 ± 9 | -323 ± 20 | -114 |
| Pulse-32 | 2.5–3.5 | -68 ± 4^a | -189 ± 4^a | -105 ± 4 | -116 ± 13 | -108 ± 7 | -88 ± 9 | | -90 |
| SMB-900 | 6–7 | -93 ± 4^b | | -124 ± 7^b | | -161 ± 9 | | | |
| SMB-900 | 32–34 | | | -363 ± 16^b | -350 ± 75 | -370 ± 93 | -321 ± 31 | | -325 |
| Bermuda Rise | | | | | | | | | |
| | | Planktonic foraminifera | Alkenone | GDGTs 0–3 | Crenarchaeol + crenarchaeol Isomer | | All GDGTs | Abundance-weighted GDGT average | |
| BC9C | 1–2 | -66 ± 3^c | -471 ± 12^c | | | | -163 ± 16 | -163 | |
| BC9C | 3–4 | -93 ± 4^c | | | | | -228 ± 12 | -228 | |
| BC9C | 4–6 | -106 ± 3^c | -516 ± 8^c | | | | -146 ± 15 | -146 | |
| BC9 | 6–7 | | | -121 ± 18 | -140 ± 20 | | | -128 | |
| BC9 | 9–11 | -139 ± 3^c | -324 ± 8^c | -125 ± 11 | -117 ± 17 | | | -121 | |
| BC9 | 21–23 | -222 ± 4^c | -537 ± 3^c | -223 ± 11 | -215 ± 15 | | | -219 | |
| GGC5 | 192–206 | -825 ± 1^c | -890 ± 4^c | -837 ± 6 | | | | -857 | |
| GGC5 | 282–292 | -859 ± 1^c | -913 ± 5^c | -852 ± 11 | -863 ± 5 | | | -868 | |
| GGC5 | 350–360 | -863 ± 5^c | -900 ± 2^c | -866 ± 14 | -870 ± 6 | | | -866 | |
| GGC5 | 360–372 | | | | | | -866 ± 8 | -866 | |
| GPC5 | 345–355 | -829 ± 1^c | | | | | -848 ± 11 | -848 | |
| GPC5 | 907–912 | -873 ± 2^c | -936 ± 3^c | -909 ± 11 | -894 ± 8 | | | -901 | |
| GPC5 | 1244–1260 | -913 ± 1^c | -927 ± 6^c | -928 ± 6 | -929 ± 6 | | | -929 | |

^a Calculated from decay-corrected $\Delta^{14}\text{C}$ values reported in Pearson et al. (2000).

^b Calculated from f_{MC} reported in Mollenhauer et al. (2007).

^c Calculated from radiocarbon ages reported in Ohkouchi et al. (2002).

Table 3
Mixing model parameter values for surface (0–75 m) and deep (75–900 m) cases

| Parameter | Post-bomb (‰) | Pre-bomb (‰) |
|---|---------------|---------------|
| 0–75 m $\Delta_{\text{water column}}$ | +63 | –81 |
| 75–900 m $\Delta_{\text{water column}}^a$ | –89 | –120 |
| Δ_{GDGTs}^b | -101 ± 13 | -116 ± 10 |

^a Post-bomb: depth-integrated average from DIC profile for WOCE station 10 line P17C. Pre-bomb values integrated from profile with upper 400 m values adjusted to reflect pre-bomb conditions.

^b Post-bomb and pre-bomb measurement error averaged to estimate uncertainty.

$\Delta^{14}\text{C}$ value of the pre-aged component is remarkably similar to the $\Delta^{14}\text{C}$ content of deep basin DIC.

Based on these mass-balance calculations, GDGT export from surface waters and from deeper in the water column both appear possible; but in either case, contemporary surface water cannot be the source of the vast majority of sedimenting GDGTs. This process distinguishes GDGTs from alkenones (which are necessarily surface-water derived) and could plausibly explain the overall depletion in ^{14}C compared to alkenones, as well as the poor TEX_{86} -derived temperatures at this location.

5.1.3. Contribution of GDGTs from sedimentary archaea

Active communities containing both Euryarchaeota and Crenarchaeota are found in continental margin (e.g., Vetriani et al., 1998; Inagaki et al., 2003; Sorensen and Teske, 2006) and deep sea sediments (e.g., Vetriani et al., 1999; Teske, 2006). These assemblages are a potential source of pre-aged GDGTs, as they could directly (by heterotrophs and methanogens) or indirectly (by methanotrophs or autotrophs) utilize aged sedimentary organic matter to produce membrane lipids.

GDGTs at Bermuda Rise have minimal contributions from anomalously old sources, either sedimentary or advected. However, ^{14}C -depleted GDGTs are required in Santa Monica Basin and may not be exclusively sourced to the deep water column. Another possible explanation is benthic archaeal production. Bermuda Rise sediments are carbonate-rich and organic-poor. The anoxic, richly organic environment of Santa Monica Basin sediments may in contrast support a more productive archaeal community and therefore a larger source of GDGTs produced in situ. A higher abundance of archaeal cells is found in sediments of the Peru Margin compared with the more poorly organic sediments of the Peru Basin and Equatorial Pacific (Inagaki et al., 2006; Teske, 2006), and archaeal biomass scales with total organic carbon content (Lipp et al., 2008).

To date, there appear to be no studies of the microbial community structure of Santa Monica Basin sediments. Evidence for occasional release of methane into the water column (Ward and Kilpatrick, 1993) does suggest that Euryarchaeota inhabit these sediments at depth. Although methanogenic and methanotrophic archaeal cells can be detected in non-methanogenic continental margin sediments (e.g., Inagaki et al., 2003; Parkes et al., 2007), the uncultured

able Miscellaneous Crenarchaeotal Group (MCG), South African Goldmine Euryarchaeotal Group 1 (SAGMEG-1), and the Euryarchaeotal Marine Benthic Group D (MBGD) are generally abundant near the surface of organic-rich sediments (Inagaki et al., 2003; Sorensen and Teske, 2006; Teske, 2006). These phylogenetic groups likely also dominate the assemblages of shallow Santa Monica Basin sediments. The extent to which this assumed archaeal assemblage would contribute ^{14}C -depleted GDGTs depends, in part, on the profile of membrane lipids that it produces.

Both Crenarchaeota and Euryarchaeota produce GDGTs (e.g., Koga and Morii, 2005; Schouten et al., 2007a). Although cultured strains that can synthesize tetraether compounds other than GDGT-0 appear to be limited (summarized in Schouten et al. (2007a)), production of GDGTs 0–3 by assemblages of sedimentary methanotrophic archaea has been noted (Pancost et al., 2001; Schouten et al., 2003b; Zhang et al., 2003; Bouloubassi et al., 2006; Werne and Sinninghe Damsté, 2005; Oba et al., 2006). Production of all GDGTs by mixed crenarchaeotal and euryarchaeotal communities was indicated in Peru Margin sediments (Biddle et al., 2006) and has elsewhere been shown to be abundant (Lipp et al., 2008). Meters deep into these sediments, GDGTs with attached diglycosidic polar head groups are assumed to be synthesized in situ by active cells, and these intact GDGTs have $\delta^{13}\text{C}$ values that appear to reflect incorporation of organic matter rather than methane. Similar sediment-dwelling archaea in Santa Monica Basin might contribute pre-aged GDGTs, if their carbon substrate is suitably ^{14}C -depleted.

While there may be some methane cycling in Santa Monica Basin, the $\delta^{13}\text{C}$ values of the GDGTs indicate that the majority of all GDGTs are likely to be made by autotrophic or heterotrophic archaea. The average $\delta^{13}\text{C}$ value of GDGTs in Santa Monica Basin ($-19.4 \pm 0.9\text{‰}$) is slightly lower than in Bermuda Rise sediments ($-18.6 \pm 0.6\text{‰}$), although the degree of variability may make this difference insignificant. All evidence suggests that archaeal GDGTs in Bermuda Rise predominantly originate in the water column. Therefore they probably reflect autotrophic Crenarchaeota and display a constant fractionation relative to DIC. This would result in relatively constant $\delta^{13}\text{C}$ values. The GDGTs in Santa Monica Basin could reflect mixed sources from autotrophic production in the water column and synthesis from organic substrates or ^{13}C -depleted DIC in the sediment. Assuming sedimentary archaea produce GDGTs with a $\delta^{13}\text{C}$ value of -22‰ (average between $\delta^{13}\text{C}$ values measured by FISH-SIMS and on biphytane derivatives of intact polar lipids (Biddle et al., 2006)) and GDGTs are exported from the water column with a $\delta^{13}\text{C}$ value equal to average water column GDGTs (-19‰), ~ 0 – 30% of total GDGTs in SMB could derive from heterotrophic production. This estimate is highly uncertain, however, given the small range and high uncertainty of the endmember $\delta^{13}\text{C}$ values. Regardless, a 30% source from benthic production is not enough to explain the degree of ^{14}C -depletion observed in Santa Monica Basin GDGTs, unless the planktonic fraction also comes primarily from the deeper (>75 m) water column (Section 5.1.2), and thus

both benthic production and deep-water export could be important.

Values of TEX_{86} also are highly variable in Santa Monica Basin sediments, ranging from 0.49 to 0.77 (17–32 °C). These values are anomalously warm and highly variable. Overlying sea surface temperatures range from 14 to 19 °C annually (California Cooperative Oceanic Fisheries Investigations (CalCOFI) database). TEX_{86} values calculated from suspended particulate matter collected at 25, 100, 600, and 850 m in the water column also span this temperature range ($\text{TEX}_{86} = 0.42\text{--}0.53$ or 13–19 °C; Wuchter et al., 2005; Kim et al., 2008). The POM data derive from a combination of suspended and sinking archaeal biomass, presumably including deep water column archaea, and yet cannot explain anomalous temperatures in excess of 30 °C. This suggests that at least some fraction of sedimentary GDGTs must indeed reflect marine benthic archaeal production in situ.

In subsurface sediments from the Peru Margin, the heterotrophic archaeal assemblage produces more GDGT-0 than any other GDGT; only a small amount of crenarchaeol is produced (Biddle et al., 2006). We find tentative evidence for a similar pattern in Santa Monica Basin sediments, where a small decrease in the relative abundance of crenarchaeol with depth is offset by a small increase in the relative abundance of GDGT-0 (Table EA2-1). Although there is some variability in the abundances of GDGTs in Bermuda Rise, no similar trend with depth was detected (Table EA2-1). We also find that GDGTs 0–3 show depletion in ^{14}C with depth relative to the ^{14}C content of crenarchaeol, and these differences are too large to be explained by radiocarbon decay over this short time (Table 1). GDGT-0 and GDGTs 1–3 have the most ^{14}C -enriched values near the surface, where they would be expected to have the smallest contribution from sedimentary production, but are more depleted in ^{14}C than crenarchaeol at all depths below 0.75 cm. In addition, the $\delta^{13}\text{C}$ values of crenarchaeol and GDGTs 1–3 are constant with depth, averaging $-19.0 \pm 0.1\text{‰}$, but the $\delta^{13}\text{C}$ value of GDGT-0 decreases with depth from -18.4‰ to -21.4‰ . The trends we observe in values of $\delta^{13}\text{C}$ and $\Delta^{14}\text{C}$ with depth would be consistent with significant in situ production of GDGT-0, and possibly GDGTs 1–3.

5.1.4. Contribution of GDGTs from terrestrial sources

Terrestrial material remains a final option to explain the ^{14}C anomalies among the GDGTs. Terrestrially derived *n*-alkanes and long-chain fatty acids have been detected in Santa Monica Basin (Pearson and Eglinton, 2000; Mollenhauer and Eglinton, 2007). Hwang et al. (2005) also observed that lipids are a significant fraction of the organic material delivered to the California Margin by riverine POM. Sediments of the Bermuda Rise show evidence of terrigenous input based on the abundance of clay and silt particles (Keigwin, 1996). This terrestrial material is thought to come from aeolian inputs from North America and Africa, local resuspended sediments eroded from the Bermuda Rise scarp, and more distantly from re-suspended terrigenous sediment from the Canadian Margin off Nova Scotia (Keigwin, 1996).

A large recent survey of globally distributed soils found archaeal GDGTs detectable in nearly all samples (Weijers et al., 2006, 2007). GDGTs also recently have been reported in river water (Herfort et al., 2006). This ubiquitous presence of GDGTs in continental material indicates that they may be an important component of terrigenous organic carbon, where they could become pre-aged by intermediate storage in continental reservoirs. Although the concentration of GDGTs in soils is up to two orders of magnitude lower than in marine sediments (Weijers et al., 2006), terrigenous GDGTs that are not degraded during transport to the ocean are more likely to be physically protected (e.g., associated with mineral surfaces) and less susceptible to degradation than autochthonous GDGTs exported from the surface ocean (Huguet, 2007). This input would cause the marine sedimentary GDGT pool to appear more aged.

BIT index values (Hopmans et al., 2004) were calculated to determine the influence of terrestrially derived GDGTs within the sedimentary organic matter of both Santa Monica Basin and Bermuda Rise (Table EA2-1). These values do not indicate a large terrestrial contribution of tetraethers. There is a small relative abundance of bacterial tetraethers at all depths in Bermuda Rise sediment (average BIT value is 0.12), which suggests that marine-derived material is predominant. Although branched tetraethers were only measured in one sediment horizon from Santa Monica Basin, the BIT index value (0.15) again does not indicate significant input of terrigenous GDGTs. Furthermore, there does not appear to be any relationship between the BIT index values and the magnitude of the difference between $\Delta^{14}\text{C}_{\text{GDGTs}}$ and $\Delta^{14}\text{C}_{\text{foraminifera}}$ (Tables 1 and EA2-1). We conclude that in these environments, pre-aged GDGTs from terrestrial sources are unlikely to explain ^{14}C -depleted values of GDGTs.

5.2. Crenarchaeol regioisomer and TEX_{86}

Because of its small relative abundance, it was only possible to make two individual measurements of the ^{14}C content of crenarchaeol regioisomer. However, these two samples show that this GDGT has a source or history that is different from the rest of the GDGT assemblage. In each case, the $\Delta^{14}\text{C}$ value is significantly more negative than other GDGTs from the same sediment depth: it is 159‰ depleted relative to the abundance-weighted average of other co-occurring GDGTs at 0.75–1.5 cm and 219‰ depleted at 1.5–2.5 cm.

These unusual values are not likely to result from contamination or isotopic fractionation. Any contamination occurring during the process of sample preparation would have affected all GDGTs rather than just the crenarchaeol regioisomer, and this was not observed. The addition of exogenous carbon by the GDGT extraction and isolation process has been carefully quantified (Shah and Pearson, 2007) and corrected for by isotope mass balance with full propagation of error (Section 3 and Electronic Annex EA-1). This process of blank correction has also been successfully applied to much smaller samples in which any contaminant would have caused a proportionally greater bias (e.g., all GDGTs from 32 to 34 cm in Santa Monica Basin

and all data reported in Ingalls et al. (2006)). Fractionation also cannot explain these offsets, as the value of $\delta^{13}\text{C}$ measured for crenarchaeol regioisomer (-20.6‰) is similar to other measured GDGTs. Finally, by definition, values of $\Delta^{14}\text{C}$ already are corrected for biosynthetic isotope fractionation.

The distinctively depleted ^{14}C content of crenarchaeol regioisomer is difficult to explain. Its value of $\delta^{13}\text{C}$ is not low enough to implicate sedimentary methane oxidizers. Although it is thought to be exported from the surface ocean (Schouten et al., 2002), it has been reported that crenarchaeol regioisomer is almost undetectable in the surface waters of the Black Sea (Wakeham et al., 2004) and North Central Pacific (Ingalls et al., 2006) and is not present in the cultured species, *Nitrosopumilus maritimus* (Schouten et al., 2008). In addition, marine crenarchaeal communities enriched from North Sea and Indian Ocean surface water produced minimal crenarchaeol regioisomer in incubation studies: its abundance was a factor of 14 lower than found in typical sediments (Wuchter et al., 2004; Schouten et al., 2007b).

Alternatively, it could be possible that the regioisomer is produced by isomerization of crenarchaeol during diagenesis or has a separate (benthic) biosynthetic source. Either option might accumulate greater relative quantities of crenarchaeol regioisomer in sediments of increasing age, however, and no such increase with depth is observed in either Bermuda Rise or Santa Monica Basin. Its proportion is relatively constant, although relative enrichment of the regioisomer within a particular endmember component (i.e., the benthic-derived fraction) cannot be conclusively ruled out. Another possibility is that the crenarchaeol regioisomer is particularly resistant to degradation. GDGT concentrations measured in oxic and anoxic layers of Madeira Abyssal Plain turbidite sediments suggest that the crenarchaeol regioisomer has a similar preservation efficiency as other GDGTs (Huguet, 2007). However, this comparison again assumes a uniform source and degradation history for all GDGTs and may not be conclusive. In summary, the crenarchaeol regioisomer is most probably explained by a combination of in situ sediment sources and/or isomerization during diagenesis, possibly combined with advection from distant locations. If so, these processes could affect crenarchaeol regioisomer throughout oceanic sediments. Further work is needed to investigate this possibility.

An aged or non-surficial source for crenarchaeol regioisomer has implications for paleotemperature reconstructions. Previous work empirically establishes the TEX_{86} index as a robust signal for sea surface temperature (e.g., Schouten et al., 2002; Wuchter et al., 2005, 2006), likely reflecting a biophysical adaptation (Wuchter et al., 2004; Schouten et al., 2007b). Archaea are known to increase the number of rings in their membrane lipids in response to increasing growth temperature (e.g., ?; Uda et al., 2001). In developing the TEX_{86} index, Schouten et al. (2002) noted that a formula incorporating four of the six abundant GDGTs in sediments, namely GDGTs 1–3 and the crenarchaeol regioisomer, resulted in the best correlation with annual mean sea surface temperature. Given the

^{14}C results above, the question becomes how is the anomalous crenarchaeol regioisomer accommodated within this relationship? Its isotopic composition suggests a different origin.

TEX_{86} is constructed as a ratio of GDGT abundances:

$$\text{TEX}_{86} = \frac{[\text{GDGT-2}] + [\text{GDGT-3}] + [\text{crenarchaeol regioisomer}]}{[\text{GDGT-1}] + [\text{GDGT-2}] + [\text{GDGT-3}] + [\text{crenarchaeol regioisomer}]} \quad (3)$$

With increasing temperature (i.e., increasing TEX_{86} value), the GDGT with one internal cyclopentane ring (GDGT-1) should have a smaller relative abundance compared to each individual GDGT with more rings, as well as to their sum, based on the proposed biophysical mechanism. For example, Sluijs et al. (2006) created a modified formula, TEX'_{86} , from which GDGT-3 was removed. This changes the absolute value of TEX'_{86} relative to TEX_{86} , but it does not appreciably change the overall slope of the TEX –temperature relationship. This allows paleotemperature to be calculated from TEX'_{86} with similar precision as from TEX_{86} .

For comparison, we constructed an additional modified version of the TEX_{86} index, removing the contribution of crenarchaeol regioisomer (TEX^*_{86}). TEX^*_{86} is calculated from:

$$\text{TEX}^*_{86} = \frac{[\text{GDGT-2}] + [\text{GDGT-3}]}{[\text{GDGT-1}] + [\text{GDGT-2}] + [\text{GDGT-3}]} \quad (4)$$

Similar to TEX'_{86} , removing crenarchaeol regioisomer should not significantly change the slope of the modified TEX_{86} relationship if the relationship between GDGT-1 and crenarchaeol regioisomer is analogous to the relationship between GDGT-1 and GDGT-3.

The relationships of TEX'_{86} and TEX^*_{86} to the original TEX_{86} index are illustrated in Fig. 6a and b. The three index values are calculated for our Bermuda Rise and Santa Monica Basin samples as well as for the only published study of sedimentary lipids with reported GDGT abundances (Herfort et al., 2006). The values of the modified TEX_{86} formulae are plotted against values of the original TEX_{86} formula. Removal of GDGT-3 from TEX_{86} changes the absolute value of the index, shown by the constant offset between TEX'_{86} and TEX_{86} (Fig. 6a), at a constant slope of approximately one (Fig. 6a). The role of GDGT-3 (like GDGT-1 and GDGT-2) in the TEX_{86} index follows the pattern predicted by the biophysical mechanism requiring more internal rings at higher temperatures.

The crenarchaeol regioisomer, in contrast, appears to have a different role in creating the TEX_{86} correlation with temperature. TEX^*_{86} values are offset from TEX_{86} values by a variable amount (slope = 0.69, Fig. 6b). The larger offset at higher values of TEX_{86} shows that the presence of crenarchaeol regioisomer in the original TEX_{86} formula is responsible for maintaining a steep slope, and therefore a greater sensitivity to temperature (i.e., $\Delta\text{TEX}_{86}/\Delta\text{temperature}$ is greater for TEX_{86} than for TEX^*_{86}). This certainly controls the precision with which sea surface temperatures can be reconstructed.

Crenarchaeol regioisomer appears to be a critical component of the TEX_{86} signal that is controlled differently

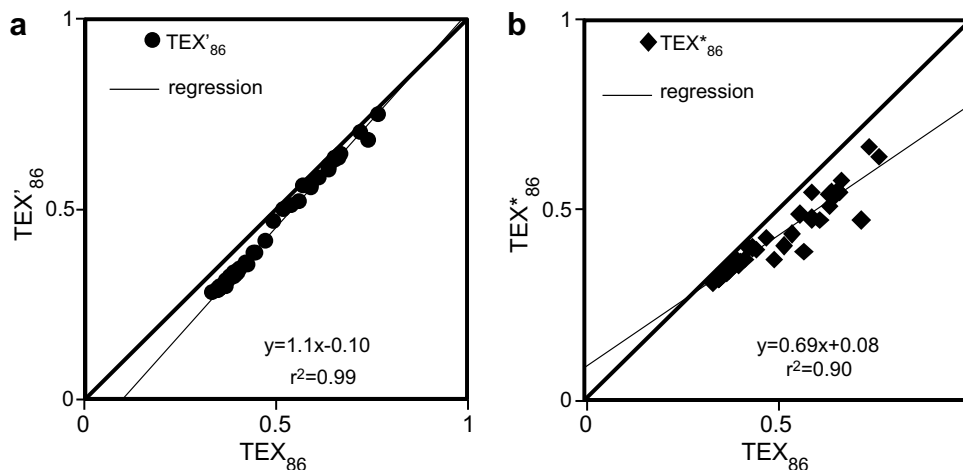


Fig. 6. (a) TEX'_{86} calculated as described in Sluijs et al. (2006) (without GDGT-3); and (d) TEX^*_{86} (without crenarchaeol regioisomer). Modified formula TEX'_{86} and TEX^*_{86} values were calculated for the Santa Monica Basin and Bermuda Rise samples reported here, as well as for values from the literature (North Sea sediments; Herfort et al., 2006).

from GDGTs 1–3, and the ^{14}C data indicate that a process other than recent export from the sea surface affects the concentration of crenarchaeol regioisomer in sediments. Finding an explanation for this ^{14}C anomaly and determining how crenarchaeol regioisomer is regulated by temperature will be essential in future studies.

6. CONCLUSIONS

Our radiocarbon measurements show that there are similarities and differences between the post-depositional processes that affect alkenones and GDGTs. Both may be affected by re-suspension from the sediment and advective transport. However, GDGTs do not appear to survive transport as well as do alkenones. Under conditions of oxic degradation within the water column, especially, evidence suggests that GDGTs are more labile and alkenones more resistant. This suggests that sedimentary alkenones are more adversely susceptible to artifacts when constructing paleo-SST records; GDGTs are more likely to be of local origin.

Conversely, it appears that sedimentary GDGT signatures more often may be subject to influences originating from below the photic zone. There may be export of GDGTs from archaea that live deeply in the water column. It also appears that deep export may not necessarily explain all of the ^{14}C -aged GDGTs found in Santa Monica Basin. Although deep production in the water column likely contributes some GDGTs, this source may not be depleted enough in ^{14}C to account for the signal observed in sediments, especially in the cases of crenarchaeol regioisomer and GDGT-0. Thus, in systems such as Santa Monica Basin there also may be a sedimentary source of anomalously old GDGTs that are produced in situ. This effect may be observed in environments that are organic rich and/or that have anoxic bottom waters or sediments and/or poor reconstructed values of temperature derived from TEX_{86} . There does not appear to be significant terrestrial input of GDGTs either to Bermuda Rise or to Santa Monica Basin,

but this should be examined in more detail in Santa Monica Basin, as only one value of the BIT index could be calculated.

One GDGT, the crenarchaeol regioisomer, appears to have a source that is different from the other five GDGTs. Its $\Delta^{14}\text{C}$ value was significantly more negative than other co-occurring GDGTs, and investigation of its contribution to the TEX_{86} index also supports an alternative origin or control on its abundance. The true source of this GDGT is unknown, but upper water column samples and archaeal cultures contain minimal or no crenarchaeol regioisomer. Understanding how and/or if these processes affect TEX_{86} paleotemperature reconstructions will be an important avenue of further investigation.

Finally, this work shows that there are multiple processes affecting the abundance and preservation of sedimentary GDGTs. The importance of each of these processes will vary according to local seafloor topography, oxygenation conditions, and sedimentary archaeal communities. A better understanding of these processes and their variability between locations will inform TEX_{86} -derived SST reconstructions and lead to a better understanding of the sources and fates of sedimentary GDGTs.

ACKNOWLEDGMENTS

We thank NOSAMS, W.J. Jenkins, A.P. McNichol, and L. Xu for collaboration on sample dilutions and for partial support of radiocarbon analyses. We thank S. Carter for laboratory assistance. We are grateful to Stuart Wakeham, Rienk Smittenberg, and Carme Huguet for their extensive and helpful reviews. This work was supported by the David & Lucille Packard Foundation and by NSF-OCE-0241363 and EAR-0311937 (to A.P.).

APPENDIX A. SUPPLEMENTARY DATA

Supplementary data associated with this article can be found, in the online version, at doi:10.1016/j.gca.2008.06.021.

REFERENCES

- Biddle J. F., Lipp J. S., Lever M. A., Lloyd K. G., Sørensen K. B., Anderson R., Fredricks H. F., Elvert M., Kelly T. J., Schrag D. P., Sogin M. L., Brenchley J. E., Teske A., House C. H. and Hinrichs K. U. (2006) Heterotrophic Archaea dominate sedimentary subsurface ecosystems off Peru. *Proc. Natl. Acad. Sci. USA* **103**, 3846–3851.
- Bouloubassi I., Aloisi G., Pancost R. D., Hopmans E. C., Pierre C. and Sinninghe Damsté J. S. (2006) Archaeal and bacterial lipids in authigenic carbonate crusts from eastern Mediterranean mud volcanoes. *Org. Geochem.* **37**, 484–500.
- Brassell S. C., Eglinton G., Marlowe I. T., Pflaumann U. and Sarnthein M. (1986) Molecular stratigraphy—a new tool for climatic assessment. *Nature* **320**, 129–133.
- Christensen C. J., Gorsline D. S., Hammond D. E. and Lund S. P. (1996) Nonannual laminations and expansion of anoxic basin-floor conditions in Santa-Monica Basin, California Borderland, over the past 4 centuries. *Mar. Geol.* **116**, 399–418.
- Conte M. H., Sicre M.-A., Rühlemann C., Weber J. C., Schulte S., Schulz-Bull D. and Blanz T. (2006) Global temperature calibration of the alkenone unsaturation index UK'37 in surface waters and comparison with surface sediments. *Geochem. Geophys. Geosyst.* **7**, Q02005. doi:10.1029/2005GC001054.
- DeLong E. F. (1992) Archaea in coastal marine environments. *Proc. Natl. Acad. Sci. USA* **89**, 5685–5689.
- DeLong E. F., Franks D. G. and Alldredge A. L. (1993) Phylogenetic diversity of aggregate-attached vs. free-living marine bacterial assemblages. *Limnol. Oceanogr.* **38**, 924–934.
- DeRosa M. and Gambacorta A. (1988) The lipids of archaeobacteria. *Prog. Lipid Res.* **27**, 153–175.
- Fuhrman J., McCallum A. and Davis A. (1992) Novel major archaeobacterial group from marine plankton. *Nature* **356**, 148–149.
- Grimalt J. O., Rullkötter J., Sicre M.-A., Summons R., Farrington J., Harvey H. R., Goñi M. and Sawada K. (2000) Modifications of the C₃₇ alkenone and alkenoate composition in the water column and sediment: possible implications for sea surface temperature estimates in paleoceanography. *Geochem. Geophys. Geosystems* **1**. doi:10.1029/2000GC000053.
- Hagadorn J. W., Stott L. D., Sinha A. and Rincon M. (1995) Geochemical and sedimentologic variations in inter-annually laminated sediments from Santa-Monica Basin. *Mar. Geol.* **125**, 111–131.
- Herfort L., Schouten S., Boon J. P. and Sinninghe Damsté J. S. (2006) Application of the TEX₈₆ temperature proxy to the southern North Sea. *Org. Geochem.* **37**, 1715–1726.
- Herndl G. J., Reinthaler T., Teira E., van Aken H., Veth C., Pernthaler A. and Pernthaler J. (2005) Contribution of Archaea to total prokaryotic production in the deep Atlantic Ocean. *Appl. Environ. Microbiol.* **71**, 2303–2309.
- Hopmans E. C., Schouten S., Pancost R. D., van der Meer M. T. J. and Sinninghe Damsté J. S. (2000) Analysis of intact tetraether lipids in archaeal cell material and sediments by high performance liquid chromatography/atmospheric pressure chemical ionization mass spectrometry. *Rapid Commun. Mass Spectrom.* **14**, 585–589.
- Hopmans E. C., Weijers J. W. H., Schefuß E., Herfort L., Sinninghe Damsté J. S. and Schouten S. (2004) A novel proxy for terrestrial organic matter in sediments based on branched and isoprenoid tetraether lipids. *Earth Planet. Sci. Lett.* **224**, 107–116.
- Huguet, C. (2007) TEX₈₆ paleothermometry: proxy validation and application in marine sediments. Ph.D. Thesis, Royal Netherlands Institute for Sea Research.
- Huguet C., Schimmelmann A., Thunell R., Lourens L. J., Sinninghe Damsté J. S. and Schouten S. (2007) A study of the TEX₈₆ paleothermometer in the water column and sediments of the Santa Barbara Basin, California. *Paleoceanography* **22**. doi:10.1029/2006PA001310.
- Hwang J., Druffel E. R. M. and Komada T. (2005) Transport of organic carbon from the California coast to the slope region: a study of specific $\Delta^{14}\text{C}$ and $\delta^{13}\text{C}$ signatures of organic compound classes. *Global Biogeochem. Cycles* **19**. doi:10.1029/2004GB002422.
- Inagaki F., Suzuki M., Takai K., Oida H., Sakamoto T., Aoki K., Neelson K. H. and Horikoshi K. (2003) Microbial communities associated with geological horizons in coastal seafloor sediments from the Sea of Okhotsk. *Appl. Environ. Microbiol.* **69**, 7224–7235.
- Inagaki F., Nunoura T., Nakagawa S., Teske A., Lever M., Lauer A., Suzuki M., Takai K., Delwiche M., Colwell F. S., Neelson K. H., Horikoshi K., D'Hondt S. and Jørgensen B. B. (2006) Biogeographical distribution and diversity of microbes in methane hydrate-bearing deep marine sediments on the Pacific Ocean Margin. *Proc. Natl. Acad. Sci. USA* **103**, 2815–2820.
- Ingalls A. E., Shah S. R., Hansman R. L., Aluwihare L. I., Santos G. M., Druffel E. R. M. and Pearson A. (2006) Quantifying archaeal community autotrophy in the mesopelagic ocean using natural radiocarbon. *Proc. Natl. Acad. Sci. USA* **103**, 6442–6447.
- Karner M. B., DeLong E. F. and Karl D. M. (2001) Archaeal dominance in the mesopelagic zone of the Pacific Ocean. *Nature* **409**, 507–510.
- Keigwin L. D. (1996) The little ice age and medieval warm period in the Sargasso Sea. *Science* **274**, 1504–1508.
- Kim J. H., Schouten S., Hopmans E. C., Donner B. and Sinninghe Damsté J. S. (2008) Global sediment core-top calibration of the TEX₈₆ paleothermometer in the ocean. *Geochim. Cosmochim. Acta* **72**, 1154–1173.
- Koga Y. and Morii H. (2005) Recent advances in structural research on ether lipids from archaea including comparative and physiological aspect. *Biosci. Biotechnol. Biochem.* **69**, 2019–2034.
- Könneke M., Bernhard A. E., de la Torre J., Walker C. B., Waterbury J. B. and Stahl D. A. (2005) Isolation of an autotrophic ammonia-oxidizing marine archaeon. *Nature* **437**, 534–546.
- Kuypers M. M. M., Blokker P., Erbacher J., Kinkel H., Pancost R. D., Schouten S. and Sinninghe Damsté J. S. (2002) Archaeal remains dominate marine organic matter from the early Albian oceanic anoxic event 1b. *Palaeogeogr. Palaeoclimatol. Palaeoecol.* **185**, 211–234.
- Lipp J. S., Morono, Y., Inagaki, F. and Hinrichs, K. U. (2008). Archaea dominate prokaryotic biomass in the deep marine subsurface. *Nature*, doi:10.1038/nature07174.
- Marlowe I. T., Green J. C., Neal A. C., Brassell S. C., Eglinton G. and Course P. A. (1984) Long-chain (*n*-C₃₇–C₃₉) alkenones in the prymnesiophyceae—distribution of alkenones and other lipids and their taxonomic significance. *Br. Phycol. J.* **19**, 203–216.
- Mollenhauer G. and Eglinton T. I. (2007) Diagenetic and sedimentological controls on the composition of organic matter preserved in California Borderland Basin sediments. *Limnol. Oceanogr.* **52**, 558–576.
- Mollenhauer G., Eglinton T. I., Ohkouchi N., Schneider R. R., Müller P. J., Grootes P. M. and Rullkötter J. (2003) Asynchronous alkenone and foraminifera records from the Benguela Upwelling System. *Geochim. Cosmochim. Acta* **67**, 2157–2171.
- Mollenhauer G., Kienast M., Lamy F., Meggers H., Schneider R. R., Hayes J. M. and Eglinton T. I. (2005) An evaluation of C-14

- age relationships between co-occurring foraminifera, alkenones, and total organic carbon in continental margin sediments. *Paleoceanography* **20**. doi:10.1029/2004PA001103.
- Mollenhauer G., Inthorn M., Vogt T., Zabel M., Sinninghe Damsté J. S. and Eglinton T. I. (2007) Aging of marine organic matter during cross-shelf lateral transport in the Benguela upwelling system revealed by compound-specific radiocarbon dating. *Geochem. Geophys. Geosystems* **8**. doi:10.1029/2007GC001603.
- Oba M., Sakata S. and Tsunogai U. (2006) Polar and neutral isopranyl glycerol ether lipids as biomarkers of archaea in near-surface sediments from the Nankai Trough. *Org. Geochem.* **37**, 1643–1654.
- Ohkouchi N., Eglinton T. I., Keigwin L. D. and Hayes J. M. (2002) Spatial and temporal offsets between proxy records in a sediment drift. *Science* **298**, 1224–1227.
- Ohkouchi N., Xu L., Reddy C. M., Montluçon D. and Eglinton T. I. (2005) Radiocarbon dating of alkenones from marine sediments: I. Isolation protocol. *Radiocarbon* **47**, 401–412.
- Pancost R. D., Hopmans E. C. and Sinninghe Damsté J. S. and the MEDINAUT Shipboard Scientific Party (2001) Archaeal lipids in Mediterranean cold seeps: molecular proxies for anaerobic methane oxidation. *Geochim. Cosmochim. Acta* **65**, 1611–1627.
- Parkes R. J., Cragg B. A., Banning N., Brock F., Webster G., Fry J. C., Hornibrook E., Pancost R. D., Kelly S., Knab N., Jørgensen B. B., Rinna J. and Weightman A. J. (2007) Biogeochemistry and biodiversity of methane cycling in subsurface marine sediments (Skagerrak, Denmark). *Environ. Microbiol.* **9**, 1146–1161.
- Pearson A. and Eglinton T. I. (2000) The origin of n-alkanes in Santa Monica Basin surface sediment: a model based on compound-specific $\Delta^{14}\text{C}$ and $\delta^{13}\text{C}$ data. *Org. Geochem.* **31**, 1103–1116.
- Pearson A., McNichol A. P., Schneider R. J., Von Reden K. F. and Zheng Y. (1998) Microscale AMS ^{14}C measurement at NOSAMS. *Radiocarbon* **40**, 61–75.
- Pearson A., Eglinton T. I. and McNichol A. P. (2000) An organic tracer for surface ocean radiocarbon. *Paleoceanography* **15**, 541–550.
- Pearson A., McNichol A. P., Benitez-Nelson B. C., Hayes J. M. and Eglinton T. I. (2001) Origins of lipid biomarkers in Santa Monica Basin surface sediment: a case study using compound-specific $\Delta^{14}\text{C}$ analysis. *Geochim. Cosmochim. Acta* **65**, 3123–3137.
- Sachs J. P. and Lehman S. J. (1999) Subtropical North Atlantic temperatures 60,000–30,000 years ago. *Science* **286**, 756–759.
- Schouten S., Hopmans E. C., Schefuß E. and Sinninghe Damsté J. S. (2002) Distributional variations in marine crenarchaeal membrane lipids: a new tool for reconstructing ancient sea water temperatures? *Earth Planet. Sci. Lett.* **204**, 265–274.
- Schouten S., Hopmans E. C., Forster A., van Breugel Y., Kuypers M. M. M. and Sinninghe Damsté J. S. (2003a) Extremely high sea-surface temperatures at low latitudes during the middle Cretaceous as revealed by archaeal membrane lipids. *Geology* **31**, 1069–1072.
- Schouten S., Wakeham S. G., Hopmans E. C. and Sinninghe Damsté J. S. (2003b) Biogeochemical evidence that thermophilic archaea mediate the anaerobic oxidation of methane. *Appl. Environ. Microbiol.* **69**, 1680–1686.
- Schouten S., Hopmans E. C. and Sinninghe Damsté J. S. (2004) The effect of maturity and depositional redox conditions on archaeal tetraether lipid palaeothermometry. *Org. Geochem.* **35**, 567–571.
- Schouten S., van der Meer M. T. J., Hopmans E. C., Rijpstra W. I. C., Reysenbach A. L., Ward D. M. and Sinninghe Damsté J. S. (2007a) Archaeal and bacterial glycerol dialkyl glycerol tetraether lipids in hot springs of Yellowstone National Park. *Appl. Environ. Microbiol.* **73**, 6181–6191.
- Schouten S., Forster A., Panoto E. and Sinninghe Damsté J. S. (2007b) Towards calibration of the TEX₈₆ paleothermometer for tropical sea surface temperatures in ancient greenhouse worlds. *Org. Geochem.* **38**, 1537–1546.
- Schouten S., Hopmans E. C., Baas M., Boumann H., Standfest S., Konneke M., Stahl D. A. and Sinninghe Damsté J. S. (2008) Intact membrane lipids of “Candidatus Nitrosopumilus maritimus,” a cultivated representative of the cosmopolitan mesophilic group I crenarchaeota. *Appl. Environ. Microbiol.* **74**, 2433–2440.
- Shah S. R. and Pearson A. (2007) Ultra-microscale (5–25 μgC) analysis of individual lipids by ^{14}C AMS: assessment and correction for sample processing blanks. *Radiocarbon* **49**, 69–82.
- Sinninghe Damsté J. S., Rijpstra W. I. C. and Reichart G. J. (2002a) The influence of oxic degradation on the sedimentary biomarker record II. Evidence from Arabian Sea sediments. *Geochim. Cosmochim. Acta* **66**, 2737–2754.
- Sinninghe Damsté J. S., Schouten S., Hopmans E. C., van Duin A. C. T. and Geenevasen J. A. J. (2002b) Crenarchaeol: the characteristic core glycerol dibiphytanyl glycerol tetraether membrane lipid of cosmopolitan pelagic crenarchaeota. *J. Lipid Res.* **43**, 1641–1651.
- Sluijs A., Schouten S., Pagani M., Woltering M., Brinkhuis H., Sinninghe Damsté J. S., Dickens G. R., Huber M., Reichart G. J., Stein R., Matthiessen J., Lourens L. J., Pedentchouk N., Backman J. and Moran K. (2006) Subtropical arctic ocean temperatures during the Palaeocene/Eocene thermal maximum. *Nature* **441**, 610–613.
- Smittenberg R. H., Hopmans E. C., Schouten S. and Sinninghe Damsté J. S. (2002) Rapid isolation of biomarkers for compound specific radiocarbon dating using high-performance liquid chromatography and flow injection analysis-atmospheric pressure chemical ionization mass spectrometry. *J. Chromatogr. A* **978**, 129–140.
- Sorensen K. B. and Teske A. (2006) Stratified communities of active archaea in deep marine subsurface sediments. *Appl. Environ. Microbiol.* **72**, 4596–4603.
- Stuiver M. and Polach H. A. (1977) Discussion, reporting of ^{14}C data. *Radiocarbon* **19**, 355–363.
- Teske A. P. (2006) Microbial communities of deep marine subsurface sediments: molecular and cultivation surveys. *Geomicrobiol. J.* **23**, 357–368.
- Teske A., Hinrichs K. U., Edgcomb V., Gomez A. D., Kysela D., Sylva S. P., Sogin M. L. and Jannasch H. W. (2002) Microbial diversity of hydrothermal sediments in the Guaymas Basin: evidence for anaerobic methanotrophic communities. *Appl. Environ. Microbiol.* **68**, 1994–2007.
- Tsuchiya, M. (2000) World Ocean Circulation Experiment hydrographic public data, Line P17C. Available from: <http://whpo.ucsd.edu/data/onetime/pacific/p17/p17c/index.htm>.
- Uda I., Sugai A., Itoh Y. H. and Itoh T. (2001) Variation in molecular species of polar lipids from thermoplasma acidophilum depends on growth temperature. *Lipids* **36**, 103–105.
- Vetriani C., Reysenbach A. L. and Dore J. (1998) Recovery and phylogenetic analysis of archaeal rRNA sequences from continental shelf sediments. *FEMS Microbiol. Lett.* **161**, 83–88.
- Vetriani C., Jannasch H. W., MacGregor B. J., Stahl D. A. and Reysenbach A. L. (1999) Population structure and phylogenetic characterization of marine benthic archaea in deep-sea sediments. *Appl. Environ. Microbiol.* **65**, 4375–4384.
- Wakeham S. G., Peterson M. L., Hedges J. I. and Lee C. (2002) Lipid biomarker fluxes in the Arabian Sea, with a comparison

- to the equatorial Pacific Ocean. *Deep Sea Res. Part II* **49**, 2265–2301.
- Wakeham S. G., Lewis C. M., Hopmans E. C., Schouten S. and Sinninghe Damsté J. S. (2003) Archaea mediate anaerobic oxidation of methane in deep euxinic waters of the Black Sea. *Geochim. Cosmochim. Acta* **67**, 1359–1374.
- Wakeham S. G., Hopmans E. C., Schouten S. and Sinninghe Damsté J. S. (2004) Archaeal lipids and anaerobic oxidation of methane in euxinic water columns: a comparative study of the Black Sea and Cariaco Basin. *Chem. Geol.* **205**, 427–442.
- Ward B. B. and Kilpatrick K. A. (1993) Methane oxidation associated with mid-depth methane maxima in the Southern California Bight. *Cont. Shelf Res.* **13**, 1111–1122.
- Weijers J. W. H., Schouten S., Spaargaren O. C. and Sinninghe Damsté J. S. (2006) Occurrence and distribution of tetraether membrane lipids in soils: implications for the use of the TEX₈₆ proxy and the BIT index. *Org. Geochem.* **37**, 1680–1693.
- Weijers J. W. H., Schouten S., van den Donker J. C., Hopmans E. C. and Sinninghe Damsté J. S. (2007) Environmental controls on bacterial tetraether membrane lipid distribution in soils. *Geochim. Cosmochim. Acta* **71**, 703–713.
- Werne J. P. and Sinninghe Damsté J. S. (2005) Mixed sources contribute to the molecular isotopic signature of methane-rich mud breccia sediments of Kazan mud volcano (eastern Mediterranean). *Org. Geochem.* **36**, 13–27.
- Woebken D., Fuchs B. A., Kuypers M. M. M. and Amann R. (2007) Potential interactions of particle-associated annamox bacteria and archaeal partners in the Namibian upwelling system. *Appl. Environ. Microbiol.* **73**, 4648–4657.
- Wuchter C., Schouten S., Boschker H. T. S. and Sinninghe Damsté J. S. (2003) Bicarbonate uptake by marine Crenarchaeota. *FEMS Microbiol. Lett.* **219**, 203–207.
- Wuchter C., Schouten S., Coolen M. J. L. and Sinninghe Damsté J. S. (2004) Temperature-dependent variation in the distribution of tetraether membrane lipids of marine Crenarchaeota: implications for TEX₈₆ paleothermometry. *Paleoceanography* **19**. doi:10.1029/2004PA001041.
- Wuchter C., Schouten S., Wakeham S. G. and Sinninghe Damsté J. S. (2005) Temporal and spatial variation in tetraether membrane lipids of marine Crenarchaeota in particulate organic matter: implications for TEX₈₆ paleothermometry. *Paleoceanography* **20**. doi:10.1029/2004PA001110.
- Wuchter C., Schouten S., Wakeham S. G. and Sinninghe Damsté J. S. (2006) Archaeal tetraether membrane lipid fluxes in the northeastern Pacific and the Arabian Sea: implications for TEX₈₆ paleothermometry. *Paleoceanography* **21**. doi:10.1029/2006PA001279.
- Zhang C. L., Pancost R. D., Sassen R., Qian Y. and Macko S. A. (2003) Archaeal lipid biomarkers and isotopic evidence of anaerobic methane oxidation associated with gas hydrates in the Gulf of Mexico. *Org. Geochem.* **34**, 827–836.

Associate editor: Carol Arnosti